WSRC-STI-2008-00285

KEY WORDS:
Distribution Coefficient, Solubility, Stochastic Modeling, Variability, Heterogeneity, Americium, Cadmium, Cesium, Cerium, Cobalt, Mercury, Strontium, Tin, Yttrium

RETENTION:
Permanent

DISTRIBUTION OF SORPTION COEFFICIENTS (K_d VALUES) IN THE SRS SUBSURFACE ENVIRONMENT

Kelly P. Grogan[(a)]
Robert A. Fjeld[(a)]
Daniel I. Kaplan
Gene P. Shine
Timothy A. DeVol[(a)]
John Coates[(a)]
John Seaman[(b)]

JUNE 30, 2008

[(a)] Clemson University, Environmental Engineering and Earth Sciences, Clemson, SC

[(b)] **Savannah River Ecology Laboratory, University of Georgia, Aiken, SC**

Savannah River National Laboratory
Washington Savannah River Company
Savannah River Site
Aiken, SC 29808

Prepared for the U.S. Department of Energy Under
Contract Number DE-AC09-96SR18500

DISCLAIMER

Printed in the United States of America

Prepared For
U.S. Department of Energy

KEY WORDS:
Distribution Coefficient, Solubility, Stochastic Modeling, Variability, Heterogeneity, Americium, Cadmium, Cesium, Cerium, Cobalt, Mercury, Strontium, Tin, Yttrium

RETENTION:
Permanent

DISTRIBUTION OF SORPTION COEFFICIENTS (K_d VALUES) IN THE SRS SUBSURFACE ENVIRONMENT

Kelly P. Grogan[(a)]
Robert A. Fjeld[(a)]
Daniel I. Kaplan
Gene P. Shine
Timothy A. DeVol[(a)]
John Coates[(a)]
John Seaman[(b)]

JUNE 30, 2008

[(a)] Clemson University, Environmental Engineering and Earth Sciences, Clemson, SC

[(b)] **Savannah River Ecology Laboratory, University of Georgia, Aiken, SC**

Savannah River National Laboratory
Washington Savannah River Company
Savannah River Site
Aiken, SC 29808

Prepared for the U.S. Department of Energy Under Contract Number DE-AC09-96SR18500

REVIEWS AND APPROVALS

Kelly P. Grogan, Co-author: Clemson Univ., Environmental Engin. & Earth Sci. Date

Robert A. Fjeld, Co-author: Clemson Univ., Environmental Engin. & Earth Sci. Date

6/18/2008

Daniel I. Kaplan, Co-author, SRNL Environmental & Chemical Processing Techno. Date

Gene P. Shine, Co-author, SRNL Statistical Consulting Section Date

Timothy A. DeVol, Co-author: Clemson Univ., Environmental Engin. & Earth Sci. Date

John Seaman, Co-author, Savannah River Ecology Laboratory, Univ. of Georgia Date

John Coates, Co-author, Co-author: Clemson Univ., Environ. Engin. & Earth Sci. Date

Kimberly Roberts, Peer Reviewer, SRNL Environ. & Chem. Processing Techno. Date

B. Thomas Butcher, Level 4 Manager, Waste Processing Technology Date

TABLE OF CONTENTS

LIST OF FIGURES

LIST OF TABLES

1.0 EXECUTIVE SUMMARY

Stochastic modeling is being used in the Performance Assessment program to provide a probabilistic estimate of the range of risk that buried waste may pose. The objective of this project was to collect field samples and make K_d measurements (*i.e.*, a ratio of the radionuclide concentration on soil to the concentration in water) that would provide information about the range and distribution (e.g., normal, log-normal) of K_d values for use in the Performance Assessment program. Our approach was to collect 27 depth-discrete sediment samples from a single E-Area borehole (BGO-3A), measure eight radionuclide K_d values from each sample in triplicate, and use the resulting data to estimate the statistical range and distribution of the K_d values. Using the eight radionuclides as analogues, a table will be created containing ~50 radionuclides of interest to the Performance Assessment. This report is a collaborative effort of the Savannah River National Laboratory, Clemson University, and the Savannah River Ecology Laboratory, and is taken from the thesis of Kelly Grogan, Clemson University.[1]

A ranking of the isotopes by

$\underline{K_d \text{ value magnitude was}}$: $^{241}Am/^{139}Ce/^{88}Y >> ^{57,60}Co > ^{109}Cd > ^{203}Hg > ^{137}Cs >> ^{85}Sr$.

For a given radionuclide, there was considerable variability across the depth of the entire core, typically ranging over one to two orders of magnitude. The data were also analyzed for each of three hydrostratigraphic units: the Upper Vadose Zone (3.3 to 9.8 m depth), the Lower Vadose Zone (9.8 to 16.5 m depth), and the Aquifer Zone (16.5 to 30.2 m depth). These zones are consistent with the hydrostratigraphic units identified and modeled/descretized in recent Performance Assessments. The Upper Vadose Zone generally consisted of more fine grain particles (silt and clay sized particles) than the Lower Vadose Zone, which consisted of remarkably uniform sand-sized particles. The Aquifer Zone consisted of large zones of sandy texture sediment that was interstratified with several thin clayey layers. Not surprisingly, the ranking of the hydrostratigraphic units by

$\underline{K_d \text{ variability was}}$: Aquifer Zone > Upper Vadose Zone > Lower Vadose Zone.

The 95% confidence level for the mean was approximately twice the mean in the Aquifer Zone, equal to the mean for the Upper Vadose Zone, and half the mean for the Lower Vadose Zone. Furthermore, a ranking of the hydrostratigraphic unit by

$\underline{\text{magnitude of } K_d \text{ values was}}$: Aquifer Zone > Upper Vadose Zone > Lower Vadose Zone,

suggesting that unique K_d values may be warranted for each hydrostratigraphic units.

In terms of the distributions of K_d values, when the core was taken as a whole, all of the radionuclides were most closely log-normally distributed. In the Lower Vadose Zone all of the radionuclides were most closely normally distributed. In the Upper Vadose and Aquifer Zones, the distributions varied by element and in some cases it was not possible to

[1] Grogan, K. 2008. Spatial Variability of Radionuclide Distribution Coefficients at the Savannah River Site and the Sub-surface Transport Implications. M.S. Thesis. Clemson University, Clemson, SC.

distinguish between the two distributions. However, there was a tendency for the radionuclides with greater K_d values to have normally distributions and for the radionuclides with the lesser K_d values to have a log-normal or unidentifiable distribution.

The 95-percentile range and type of distributions assigned to radionuclide K_d values should be assigned based on the following general rules. These general rules are derived from the measurements described in this report, some geochemical/geological consideration, and parsimony.

- The 95% confidence level for the mean K_d was twice the mean in the Aquifer Zone, equal to the mean for the Upper Vadose Zone, and half the mean for the Lower Vadose Zone.
- The distribution of K_d values was log normal in the Upper Vadose Zone and Aquifer Zone, and normal in the Lower Vadose Zone.

Preliminary reports that did not have site-specific data and written with the expressed purpose to provide early guidance for data input to Monte Carlo simulations generally had appreciably greater 95% confidence ranges (Kaplan and Millings 2006, Shine 2007). This is the first report of radionuclide K_d variability in the literature. This data supports the assignment of unique ranges and distributions of radionuclide K_d values by hydrostratigraphic unit. Perhaps more importantly, it supports the use of more narrow ranges of K_d values (0.5x, 1x, & 2x the mean) compared to using the distributions measured in the entire subsurface region of interest (1 to 2 orders of magnitude of the mean). Using ranges and distribution coefficients that are specific to the hydrostratigraphic unit will improve model accuracy and reduces model uncertainty.

2.0 INTRODUCTION

An important aspect of contemporary risk assessment is consideration of the variability of risk assessment parameters spatially, temporally, or across populations. Due to their variability, parameters are often more appropriately characterized by distributions rather than by single values. Risk is often quantified discretely; either by a probability for stochastic effects or by a hazard index for deterministic effects. However, due to the inherent variability of risk assessment parameters and uncertainties, risk is more appropriately characterized by a distribution. The distribution of risk due to parameter variability is calculated by propagating parameter distributions through the contaminant release, transport, exposure, and consequence assessment steps of the risk calculation process. This is typically accomplished using Monte Carlo methods, and the process is sometimes referred to as stochastic modeling. Specification of parameter distributions is thus a critical aspect of stochastic modeling. These parameters may include a mean, range, and distribution shape (e.g., normal or log-normal).

The primary means utilized for Low-Level Radioactive Waste disposal at the Savannah River Site's (SRS) E-Area is shallow-land burial. The burial grounds include low-activity waste vaults, intermediate-level vaults, engineered trenches, slit trenches, and components-in-grout trenches. These vaults and trenches are used to store many different types of Low Level Radioactive Waste including paper, plastics, wood, cloth, spent ion exchange resins, metal, concrete debris, and glass.

As part of its regulatory compliance program, SRS must perform risk analyses, or performance assessments, of its Low-Level Radioactive Waste disposal activities at E-Area. Given the variety of different soil lenses that are present at different depths below the surface of the E-Area burial grounds, the degree to which any given radionuclide sorbs within the system as a whole is largely unknown. Without the benefit of site-specific data, risk analyses and performance assessments regarding sub-surface radionuclide contaminants can be uncertain undertakings. With that in mind, one of the most important risk assessment parameters for contaminant transport from these buried wastes is the soil-water distribution coefficient, K_d, for the sediments in immediate contact with the radionuclide in groundwater. This K_d is defined as the equilibrium concentration of a radionuclide in the solid phase divided by the concentration of that same radionuclide in the aqueous phase. The value of this coefficient allows for estimation of the contaminant velocity relative to the ground water velocity and thus allows for calculation of contaminant travel time to a point of compliance.

2.1 VARIABILITY AND UNCERTAINTY ANALYSIS

Modeling of the type used in risk assessment is subject to two types of uncertainty in the parameters that are used to quantify the various physical, chemical, or biological processes that are being modeled. These are aleatory uncertainty and epistemic uncertainty. Aleatory uncertainty is related to chance, and it refers to the variability of parameters that occur over time, space or across a population (Fjeld et al., 2007). Epistemic uncertainty is related to limitations of knowledge. These limitations may include uncertainty related to the completeness of a model, uncertainty in the distributions associated with parameter variability, and a lack of available data. Whereas an aleatory uncertainty analysis yields a risk distribution, an epistemic uncertainty analysis yields confidence limits on that

distribution. Aleatory uncertainty (i.e. variability) is determined by propagating parameter distributions through a risk assessment model. This is usually accomplished using standard Monte Carlo techniques. The determination of epistemic uncertainty is a much more complex problem. Monte Carlo techniques can be combined with expert judgment to evaluate the epistemic uncertainty in variability distributions, but methods have not been established for evaluating epistemic uncertainty in models.

Aleatory uncertainty of a parameter requires measurement data, either from the laboratory or the field. The distribution of these data can be expressed in tabular form, can be empirically fit, or can be approximated by theoretical distributions. Theoretical distributions often used for approximating risk assessment parameters are uniform, normal, log-normal, and beta. Bayesian updating may also be used with regional or generic distributions as the prior (Meyer et al. 1997). Finally, a combination of methods may be used for parameter distribution determination (EPA 2001).

2.2 PREVIOUS WORK

Due to project schedule, some modeling was started prior to collecting the necessary field and laboratory data needed to fully populate SRS stochastic models (Kaplan and Millings 2006, Shine 2007). For this interim period, the project relied on generalized guidance from the literature (Wieland and Van Loon 2003) and some statistical analyses of literature data (Kaplan et al. 1998). The following early guidance was provided:

- Set the range to an order of magnitude for radionuclides with K_d values >1000 mL/g and to a factor of two for K_d values of <1000 mL/g. This decision is based on the literature.
- Set the range to an order of magnitude for radionuclides with K_{sp} values $<10^{-6}$ *M* and to a factor of two for K_d values of $>10^{-6}$ *M*. This decision is based on the literature.
- The distribution of K_d values with a mean >1000 mL/g will be log-normally distributed. Those with a K_d value <1000 mL/g will be assigned a normal distribution. This is based on statistical analysis of non-site-specific data.

Results from this study, which includes site-specific field/laboratory research involving E-Area sediments, will supersede this early guidance.

2.3 OBJECTIVES

The objective of this research was to evaluate the range and distribution of K_d values in E-Area. The approach we took was to measure radionuclide K_d values for 27 sediment samples collected from E-area and to assess the K_d value range and distribution characteristics. The specific objectives of this research were as follows:

1. to measure distribution coefficients for ^{241}Am, ^{109}Cd, ^{139}Ce, ^{57}Co, ^{60}Co, ^{137}Cs, ^{203}Hg, ^{85}Sr, and ^{88}Y in E-Area SRS sediment;
2. to characterize the distribution of these K_d values in the E-Area sediments; and
3. to conduct simple and multiple regression analyses between K_d values and sediment properties (pH, total Fe/Al/Ti, dithionite extractable Fe/Al/Ti, clay content, and cation exchange capacity).

3.0 MATERIALS AND METHODS

A detailed description of the materials and methods are presented in Appendix A. Following is a brief description, sufficient to permit understanding the results. Field sediment sampling was conducted by SRNL personnel. K_d measurements and sediment characterization was conducted by Clemson University personnel. X-ray Diffraction (XRD) analyses and Inductively Coupled Plasma – Mass Spectroscopy (ICP-MS) was conducted by University of Georgia personnel. Statistical analyses were conducted by SRNL and Clemson University personnel.

3.1 K_d VALUE MEASUREMENTS AND SEDIMENT CHARACTERIZATION

Sediment samples were collected from a single borehole (BGO-3A) located in an uncontaminated portion of E-Area. 27 depth-discrete samples were collected from depths ranging from 11 ft (3.3m) to 100 ft (30.5m) below ground surface.[2] K_d values of eight radionuclides were determined in triplicate of the 27 sediment samples by measuring the radionuclide concentration in the aqueous and solid phases. Additionally, several dozen positive and negative control samples were included in these experiments. Several sediment properties were also measured to determine if correlations could be made between the K_d values and sediment properties. The sediment properties measured were pH, total Fe/Al/Ti (as measured by X-ray Fluorescence; XRF), dithionite extractable Fe/Al/Ti (the approximate Fe, Al, and Ti concentrations in the oxyhydroxide coatings of sediment particles), clay content, and cation exchange capacity.

3.2 STATISTICAL ANALYSES

Cumulative distribution graphs of the K_d data were constructed for each radionuclide for the whole core and for each of the three subsurface strata: the Upper Vadose Zone, the Lower Vadose Zone, and the Aquifer Zone. These data were displayed in the form of probability and log-probability plots, which linearize normal and log-normal distributions, respectively. This permitted visual identification of the distributions which might be approximated as either normal or log-normal. Skewness and kurtosis were also determined for each distribution. A positive kurtosis indicated a curve with a longer tail than normal whereas a negative kurtosis indicated a curve that was flatter than normal. A positive skewness indicated tailing of the curve to the right whereas a negative skewness indicated tailing of the curve to the left.

Simple and multiple regression analyses were conducted between the various K_d values and the sediment characterization parameters. And again, additional details of the statistical methods used in the study are described in Appendix A.

[2] Grogan (2008) collected 32 samples, 27 from borehole BGO-3A, and 5 other samples not relevant to K_d distributions.

4.0 RESULTS AND DISCUSSION

4.1 SOIL CHARACTERIZATION

A sub-surface profile for the BGO-3A core is shown in Figure 1. A summary of the soil characterization data collected for the soil samples from this core is presented in Table 1. The sub-surface profile shown in Figure 1 illustrates the presence of several different soil lenses that occur throughout the BGO-3A core. These lenses represent soil layers containing sand, clay, and various mixtures of the two. Based on this figure and beginning with the soil nearest the surface, the upper portion of the core from approximately 11 to 30 feet depth contains a relatively large amount of clay content compared to the rest of the core. Directly below this generally high-clay content region, the core consists of sediments that are generally more sandy in texture; this region reaches between 32 ft to 53 ft below the surface. 53 ft depth, is (coincidently) the water table. Below the water table, the sub-surface becomes primarily sandy once again with intermediate clay lenses down to about 100 ft below the surface where one final clay lens serves to confine the aquifer.

The presence of the various sand and clay layers is confirmed by the sediment characterization data shown in Table 1, particularly the data collected for clay content, iron content, and CEC. The soil samples collected from depths between 11 and 30 ft below the surface generally show elevated levels of clay, iron, and CEC that correspond to the green and orange layers described in Table 1. Below this region, there is a noticeable decline in the levels of CEC, clay content, and iron content down to the water table at about 53 ft which corresponds to the largely sandy region described in Table 1. Finally, below the water table, there was some significant variability in the measured clay and iron content. As was the case for the region directly above the water table, the region below the water table was expected to be primarily sandy based on Table 1. This expectation was confirmed by the generally low CEC levels that were measured for this region. However, several depths show spikes in the clay content and iron content levels that correspond with the narrow green and orange lenses shown in Table 1. For example, there is a sudden increase in clay and iron content that occurs at 70 ft below the surface. Similarly, very large spikes were measured for the bottom portion of the core (90 ft to 100 ft) which corresponds to the purple clay band described in Table 1. The results of the XRD and TGA analyses along with other soil characterization data are given in Appendix B.

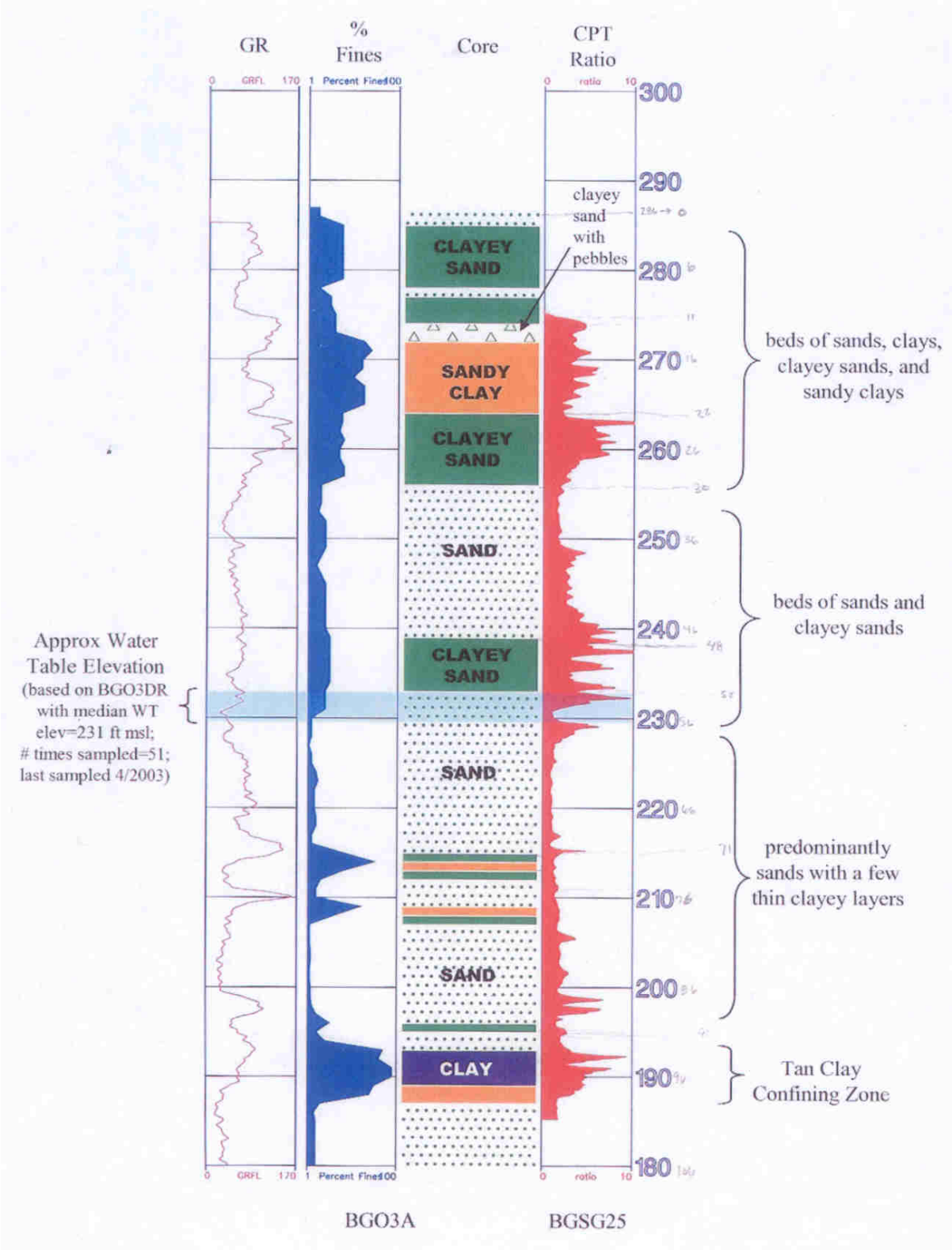

Figure 1. Sub-surface soil profile for the BGO-3A core

Table 1. Summary of soil characterization data for the BGO-3A core

Sample Depth (ft)	CEC (meq/100g)	Soil pH	Clay (wt-%)	Al [(a)] (ppm)	Ti [(a)] (ppm)	Mn [(a)] (ppm)	Fe [(a)] (ppm)
-11	2.0	5.1	21.16	1510	14	2	4272
-12.5	1.6	5.1	19.45	1424	9	2	2310
-15	2.7	6.0	29.05	1550	6	11	5062
-17.5	3.3	5.0	49.73	2168	7	4	10183
-20	1.5	4.9	18.48	1173	6	11	3554
-25	3.2	5.8	22.71	2240	15	1731	24698
-27	1.2	5.0	14.62	1255	10	18	716
-30	1.4	5.3	11.56	1104	7	27	429
-32	1.0	5.3	7.00	1237	11	7	581
-35	1.1	5.4	8.76	1525	7	9	594
-38	1.0	5.2	6.31	1601	15	12	814
-40	1.6	5.3	9.70	922	6	6	410
-42	1.0	5.2	7.16	892	4	34	209
-45	1.0	5.2	7.73	1102	6	3	260
-47	1.5	5.2	9.16	1223	12	3	327
-50	1.6	5.0	9.57	1114	7	3	253
-53	1.4	4.9	9.74	1125	6	3	288
-55	1.5	5.1	11.03	1161	8	9	363
-58	1.1	6.0	2.16	1057	24	11	1160
-60	1.0	6.4	0.31	1148	9	20	589
-70	1.6	5.0	6.60	1377	14	5	2223
-75	1.6	4.8	3.70	1291	9	5	3015
-80	1.2	6.0	2.32	1926	31	27	13619
-85	1.1	5.8	1.18	1723	16	14	6566
-90	2.9	5.3	7.94	2754	58	169	22696
-95	9.3	4.9	21.51	2498	6	204	10462
-100	7.4	5.1	12.32	1727	14	47	2991

[(a)] DCB = dithionite-citrate-buffer extractable metal; an extract that provides a measure of metals in the surface ox hydroxide coatings of soil particles and does not measure the metal content within the mineral structure such as kaolinite, quartz, and hydroxyl-interlayered vermiculite.

4.2 STATISTICAL CHARACTERIZATION OF K_d VALUES

The results of the batch sorption tests for the BGO-3A core are displayed in Figure 2. K_d values in the figure represent the median value measured for the three trials at each core depth. Values ranged from less than 1 mL/g for ^{85}Sr to greater than 1000 mL/g for ^{88}Y and ^{139}Ce. Also, there was considerable variability in the K_d values for any given radionuclide. For example, K_d values for ^{57}Co and ^{60}Co ranged from approximately 10 mL/g to over 1000 mL/g, suggesting a strong dependence of K_d on soil properties. Factors such as mineral content, cation exchange capacity, and pH are known to have a significant effect on the observed K_d for a given isotope. Error bars have been omitted from Figure 2 due to the large uncertainties that were observed for the small sample size examined (three trials) for a given sample depth. However, it is believed that the observed trends are valid because of the corresponding fluctuations that were observed for many of the isotopes. For example, ^{57}Co and ^{60}Co display almost identical mean values in their K_d profiles with depth as expected. Similar trends were noted for mercury, cadmium, and cesium as well. Sub-surface K_d profiles for the individual radionuclides along with error bars are presented in Appendix C.

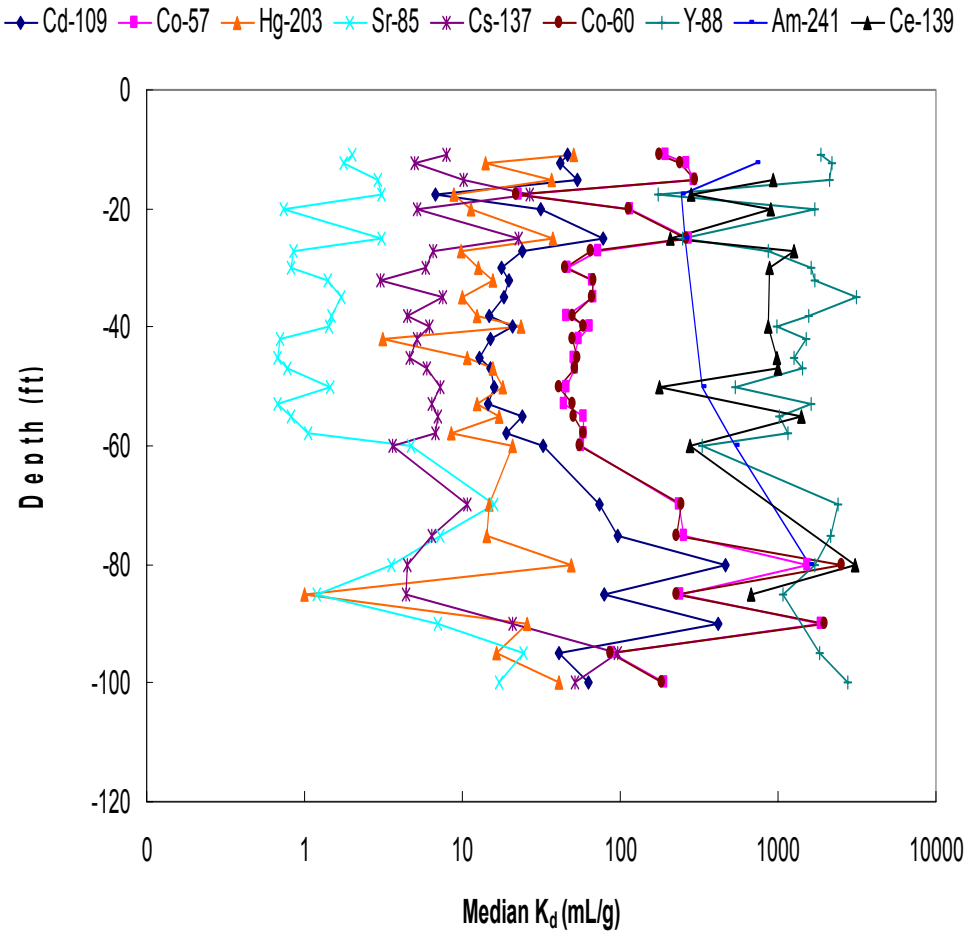

Figure 2. Sub-surface profiles of distribution coefficients of radionuclides for the BGO-3A core from the E-Area burial grounds of SRS

Summary statistics of the data are presented in Table 2. The mean for each radionuclide represents the average of 27 values, one for each depth from the BGO-3A core. These values, in turn, are the average for three samples. Values for ^{241}Am and ^{139}Ce are omitted because of the relatively small amount of data that could be collected for each of these isotopes due to their extremely low aqueous concentrations. The mean K_d values for these soils represent the lower quartile of their expected range based on the literature review. Also of note, in some cases the mean K_d value was more than a factor of four greater than the median K_d value for a given sample depth. This observation indicates that some of the mean K_d values presented in Table 2 have likely been skewed by a few very large values. The [illegible]n of the median K_d values of the radionuclides were ranked as follows:

$$^{88}Y >> ^{57,\,60}Co > ^{109}Cd > ^{203}Hg > ^{137}Cs >> ^{85}Sr.$$

Americium and cerium have not been included in this ranking because of the inability to generate enough data for sufficient statistical power.

Table 2. Compilation of summary statistics for radionuclides K_d values.

	Radionuclide						
Sample Statistic	^{109}Cd	^{137}Cs	^{57}Co	^{60}Co	^{203}Hg	^{85}Sr	^{88}Y
Mean (mL/g)	89	13	252	306	21	4.0	1641
Std. Error (mL/g)	36	3.8	84	117	3.2	1.07	139
Median (mL/g)	30	6.6	70	72	14	1.83	1573
Std. Deviation (mL/g)	185	20	436	610	17	5.6	709
Minimum (mL/g)	9.1	3.5	34	33	2.1	0.21	295
Maximum (mL/g)	927	97	1869	2710	71	23	3134

The description of the sub-surface characterization along with the sub-surface K_d profile in Figure 2 offer a means of stratifying the sample data. The variability in the median K_d value for each radionuclide was relatively small in the depth range from approximately 32 to 53 ft below the surface. This was the region described as mostly sandy and characterized by relatively constant low levels of clay content, iron content, and CEC. Above this region, where the sub-surface contained elevated levels of clay, iron, and CEC, the median K_d values displayed a moderate variability. The region below the water table showed variable levels clay, iron, and CEC and also displayed the highest relative variability in K_d. Taking these observations into consideration, three sub-surface strata were distinguished as follows: 11 – 30 ft below the surface, 32 – 53 ft below the surface, and 55 – 100 ft below the surface. These strata represent the Upper Vadose Zone, the Lower Vadose Zone, and the Aquifer

Zone, respectively. For comparison, sub-surface distribution coefficient profiles for these three strata are shown in Figure 3.

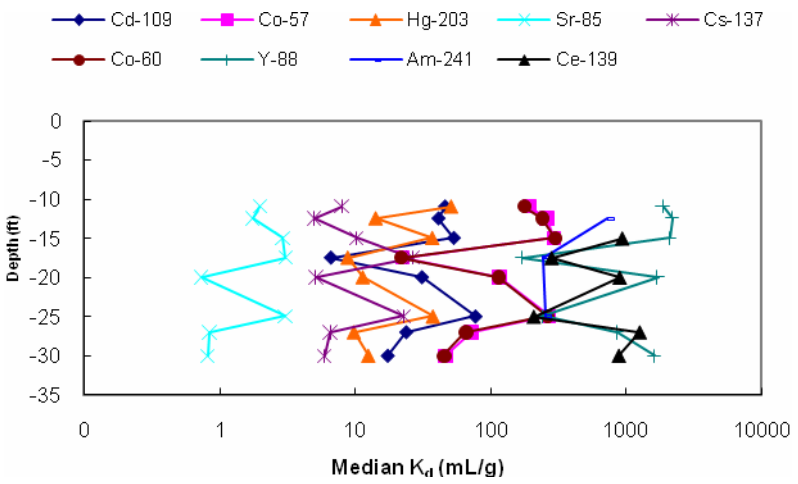

(a)

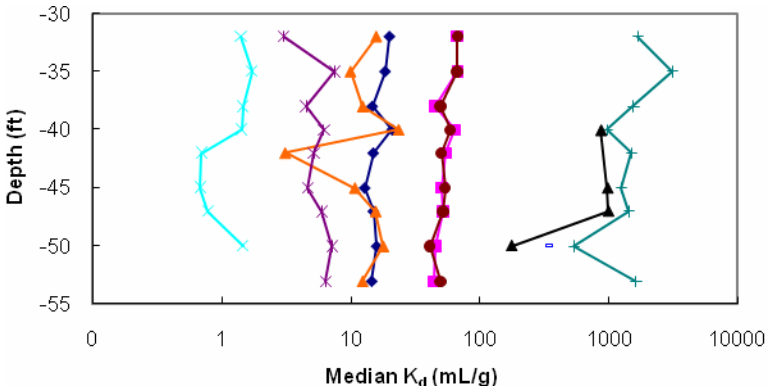

(b)

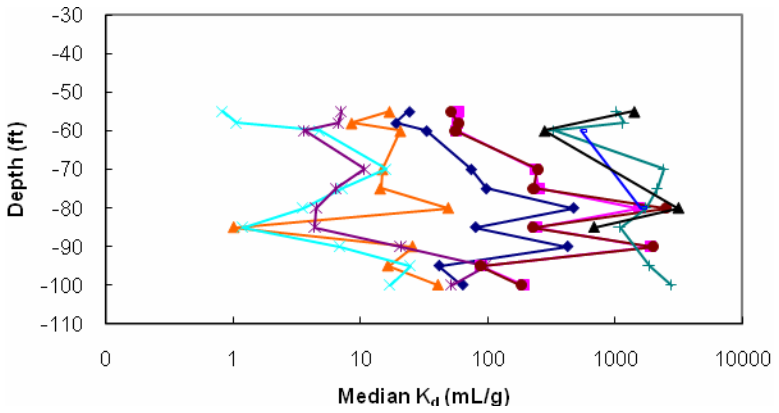

(c)

Figure 3. Sub-surface K_d profile for radionuclides in the a) Upper Vadose Zone, b) Lower Vadose Zone, and c) Aquifer Zone of the E-Area burial grounds of SRS.

The data for ^{109}Cd are summarized in Table 3 for each of the three strata. The mean and median K_d values were significantly different across the three strata. The median K_d values were 36 mL/g, 15 mL/g, and 68 mL/g for the Upper Vadose, Lower Vadose, and Aquifer Zones, respectively. Similar values were observed for the mean K_d. In both cases, the highest K_d values were measured for the Aquifer Zone, followed by the Upper Vadose Zone and the Lower Vadose Zone. Although all of these measured values fall within the range of 8 to 4,000 mL/g reported in the literature (Krupka et al. 1999), they are also all in the lower quartile of this range.

Table 3. Stratified summary statistics for K_d compiled for ^{109}Cd

Zone	Upper	Lower	Aquifer
Mean (mL/g)	37	16	131
Standard Error (mL/g)	8	0.90	53
Median (mL/g)	36	15	68
Standard Deviation (mL/g)	22	3	166
Minimum (mL/g)	7	13	19
Maximum (mL/g)	78	21	466
Number of Samples	8	9	10
Confidence Level Mean (95.0%) (mL/g)	19	2	119

Data for ^{139}Ce are presented in Table 4. Compared to the other isotopes, these results were based on fewer observations due to a number of trials having aqueous fractions of ^{139}Ce that were below detection limits. The mean and median distribution coefficient values were significantly different between the vadose Zones and the Aquifer Zone while the K_d value was relatively consistent within the two vadose Zones. The median K_d values were 888 mL/g, 926 mL/g, and 1,251 mL/g for the Upper Vadose, Lower Vadose, and Aquifer Zones respectively. In both cases, the highest K_d values were again measured for the Aquifer Zone. The Lower Vadose Zone displayed slightly higher mean and median K_d values than did the Upper Vadose Zone, but the differences seem likely to be insignificant. In this case, only Aquifer Zone K_d values for ^{139}Ce fall within the expected range of 1,050 to 1,300 mL/g based on the literature review (Ames and Rai, 1978).

Table 4. Stratified summary statistics for K_d compiled for ^{139}Ce

Zone	Upper	Lower	Aquifer
Mean (mL/g)	743	756	1364
Standard Error (mL/g)	167	195	625
Median (mL/g)	888	926	1037
Standard Deviation (mL/g)	409	390	1251
Minimum (mL/g)	210	177	277
Maximum (mL/g)	1254	993	3106
Number of Samples	6	4	4
Confidence Level Mean (95.0%) (mL/g)	429	620	1990

In terms of K_d variability, a trend similar to that of ^{109}Cd described above was observed for ^{139}Ce. The sample variance and standard deviation again increases from the Lower Vadose Zone to the Upper Vadose Zone to the Aquifer Zone, which has the highest degree of variability. Again, examining the 95% confidence levels for each zone offers additional information for early approximations of the possible variation in K_d for ^{139}Ce. In the Upper Vadose Zone, the 95% confidence level was 429 mL/g resulting in a level that was approximately one times the mean K_d of 743 mL/g in width. For the Lower Vadose Zone, the 95% confidence level was 620 mL/g which resulted in a width that was approximately two times the mean K_d of 756 mL/g. Finally, the Aquifer Zone yielded a 95% confidence level of 1,990 mL/g which was equivalent to a window equal to approximately three times the mean K_d value of 1,364 mL/g. It should be noted, however, that much of the increased width of these confidence levels was likely due to the relatively small amount of data available for ^{139}Ce. In regards to the unavailable K_d values for ^{139}Ce, these points represent samples for which the aqueous fraction was below detection limits, thus preventing an accurate determination of K_d. If these data could be included, they would likely increase the mean and median measured K_d values and decrease the width of the 95% confidence level for the mean. The amount of data `that could be collected for ^{241}was insufficient for this analyses, and thus ^{241}Am is omitted from this discussion.

The stratified data for ^{137}Cs are summarized in Table 5. The observed mean distribution coefficient values were again significantly different across the three strata. The mean K_d values were 11.3 mL/g, 5.6mL/g, and 21.2 mL/g for the Upper Vadose, Lower Vadose, and Aquifer Zones respectively. The median K_d values, however, were more consistent displaying values of 7.2 mL/g, 6.0 mL/g, and 6.9 mL/g for the Upper Vadose, Lower Vadose, and Aquifer Zones. In this case, it seems that the mean values were influenced greatly by a few extreme values. In both cases, the highest K_d values were again measured for the Aquifer Zone and Upper Vadose Zones with the Lower Vadose Zone displaying the lowest K_d values. Unlike the values collected for ^{109}Cd, not all of these values for ^{137}Cs fall within the expected range of 10 to 66,700 mL/g based on the literature review (Krupka et al. 1998). In fact, only the mean K_d values for the aquifer and Upper Vadose Zones actually fell within this range. The remaining K_d values, were below the expected range. This observation may be a result of significant differences in CEC and clay content for the soils that are typically used to evaluate distribution coefficients for ^{137}Cs compared to those soils utilized in this study.

In terms of K_d variability, a trend similar to that of ^{109}Cd described above was observed. The sample variance and standard deviation again increases from the Lower Vadose Zone to the Upper Vadose Zone to the Aquifer Zone, which has the highest degree of variability. The 95% confidence window for the mean in the Upper Vadose Zone for ^{137}Cs was 7.1 mL/g, which again was equivalent to a window with a width of about one times the mean K_d of 11 mL/g. In the Lower Vadose Zone, the 95% confidence level was 1.1 mL/g resulting in window that was approximately 0.25 times the mean K_d of 5.6 mL/g. Finally, the 95% confidence level in the Aquifer Zone was 22 mL/g which yielded a window approximately two times the mean K_d of 21 mL/g in width.

Trends similar to those described above were again identified for the stratified data from Co. In this case, in order to increase the statistical power of the data, the results from ^{57}Co and ^{60}Co were combined. The resulting summary statistics are compiled in Table 6. The

observed mean and median distribution coefficient values were again significantly different across the three strata. The median K_d values were 147 mL/g, 52 mL/g, and 207 mL/g for the upper vadose, lower vadose, and Aquifer Zones, respectively. Again, the highest K_d values were measured for the Aquifer Zone, followed by the Upper Vadose Zone, followed by the Lower Vadose Zone. Each of these measured K_d values for Co fall within the expected range of 0.03 to 12,500 mL/g based on the literature review (Cantrell et al., 2003). However, like the K_d values measured for ^{109}Cd, all of these values are in the lowest quartile of the expected range.

Table 5. Stratified summary statistics for K_d compiled for ^{137}Cs

Zone	Upper	Lower	Aquifer
Mean (mL/g)	11.3	5.6	21.2
Standard Error (mL/g)	3.0	0.5	9.5
Median (mL/g)	7.2	6.0	6.9
Standard Deviation (mL/g)	8.5	1.4	30.1
Minimum (mL/g)	5.0	3.0	3.6
Maximum (mL/g)	26.5	7.5	95.9
Number of Samples	8	9	10
Confidence Level Mean (95.0%) (mL/g)	7.1	1.1	21.5

The observed mean and median Cd K_d values were again significantly different across the three strata. The median K_d values were 147 mL/g, 52 mL/g, and 207 mL/g for the Upper Vadose, Lower Vadose, and Aquifer Zones respectively. Again, the highest K_d values were measured for the Aquifer Zone, followed by the Upper Vadose Zone, followed by the Lower Vadose Zone. Each of these measured K_d values for Co fall within the expected range of 0.03 to 12,500 mL/g based on the literature review (Cantrell et al., 2003). However, like the K_d values measured for ^{109}Cd, all of these values are in the lowest quartile of the expected range.

In terms of K_d variability, a trend similar to that of the other isotopes described above was observed. The sample variance and standard deviation again increases from the Lower Vadose Zone to the Upper Vadose Zone to the Aquifer Zone which has the highest degree of variability. Again, examination of the 95% confidence window for the mean results in the identification of ranges similar to those identified for ^{109}Cd and ^{137}Cs. In the Upper Vadose Zone, the 95% confidence level for Co was 89 mL/g which was equivalent to a window with a width of about one times the mean K_d of 154 mL/g. In the Lower Vadose Zone, the 95% confidence level was 7 mL/g resulting in a window that was approximately 0.25 times the mean K_d of 54 mL/g. Finally, the 95% confidence level in the Aquifer Zone was 597 mL/g which yielded a window approximately two times the mean K_d of 535 mL/g in width.

Table 6. Stratified summary statistics for K_d compiled for $^{57,60}Co$

Zone	Upper	Lower	Aquifer
Mean (mL/g)	154	54	535
Standard Error (mL/g)	37	3	264
Median (mL/g)	147	52	207
Standard Deviation (mL/g)	106	9	835
Minimum (mL/g)	23	44	53
Maximum (mL/g)	293	68	2273
Number of Samples	8	9	10
Confidence Level Mean (95.0%) (mL/g)	89	7	597

The results obtained from the stratified data for ^{203}Hg are somewhat different from those obtained for the previously discussed isotopes. A summary of the stratified data for ^{203}Hg is compiled in Table 7. In the case of ^{203}Hg, very little difference was observed between the mean and median K_d values across the different strata. The median K_d values were 13 mL/g, 12 mL/g, and 17 mL/g for the Upper Vadose, Lower Vadose, and Aquifer Zones respectively. In contrast to the previously discussed isotopes, the highest mean K_d was measured for the Upper Vadose Zone instead of the Aquifer Zone. The median values, however, followed the same trend as the other radionuclides in that the highest median K_d value was measured for the Aquifer Zone, followed by the upper and Lower Vadose Zones respectively. That being said, the measured values in each zone are close enough such that the differences between them are likely insignificant and the distribution coefficient for ^{203}Hg can be described as relatively constant throughout all three zones. It should be noted, however, that all of the measured values fall well below the expected K_d range of 100 to greater than 10,000 mL/g based on the literature review (Lee et al., 2001).

In terms of K_d variability, the Upper Vadose Zone and the Aquifer Zone displayed much higher standard deviations and variances compared to those of the Lower Vadose Zone. The 95% confidence windows observed for the mean also display some different trends compared to most of the other isotopes. In the Upper Vadose Zone, the 95% confidence level was 14 mL/g which corresponded to a window of about one times the mean K_d of 23 mL/g like ^{109}Cd, ^{137}Cs, and Co. The Lower Vadose Zone, however displayed a 95% confidence level of 4 mL/g which yielded a window closer to 0.6 times the mean K_d of 13 mL/g for ^{203}Hg in this zone. In the Aquifer Zone, the 95% confidence level was 10 mL/g which again resulted in window width of approximately one times the mean K_d of 21 mL/g as was the case in the Upper Vadose Zone.

Table 7. Stratified summary statistics for K_d compiled for ^{203}Hg

Zone	Upper	Lower	Aquifer
Mean (mL/g)	23	13	21
Standard Error (mL/g)	6	2	5
Median (mL/g)	13	12	17
Standard Deviation (mL/g)	16	6	14
Minimum (mL/g)	9	3	1
Maximum (mL/g)	51	23	49
Number of Samples	8	9	10
Confidence Level Mean (95.0%) (mL/g)	14	4	10

The results obtained from the stratified data for ^{85}Sr are more similar to those obtained for cadmium, cesium, and cobalt. A summary of the stratified data for ^{85}Sr is compiled in Table 8. The observed mean and median distribution coefficient values were again significantly different across the three strata. The median K_d values were 1.2 mL/g, 0.38 mL/g, and 5.1 mL/g for the Upper Vadose, Lower Vadose, and Aquifer Zones respectively. As with the other isotopes, the highest K_d values were again measured for the Aquifer Zone, followed by the Upper Vadose Zone, followed by the Lower Vadose Zone.

Table 8. Stratified summary statistics for K_d compiled for ^{85}Sr

Zone	Upper	Lower	Aquifer
Mean (mL/g)	1.90	1.15	8.32
Standard Error (mL/g)	0.36	0.14	2.58
Median (mL/g)	1.88	1.41	5.84
Standard Deviation (mL/g)	1.03	0.42	8.15
Minimum (mL/g)	0.74	0.68	0.82
Maximum (mL/g)	3.07	1.71	24.60
Count	8.00	9.00	10.00
Confidence Level (95.0%) (mL/g)	0.86	0.33	5.83

Of these measured K_d values for ^{85}Sr, only those listed for Aquifer Zone fall within the expected range of 2 to 1,600 mL/g based on the literature review (EPA 2001). The remaining values fall below this range. That being said, even the K_d values measured for the Aquifer Zone are at the bottom of the expected range.

In terms of K_d variability, a trend similar to that of the other isotopes described above was observed. The sample variance and standard deviation again increases from the Lower Vadose Zone to the Upper Vadose Zone to the Aquifer Zone which has the highest degree of variability. In the case of strontium, the 95% confidence windows for the mean display similar trends to those of cadmium, cesium, and cobalt in the Upper Vadose and Aquifer Zones. A different observation, however, is made for the Lower Vadose Zone compared to those isotopes. In the Upper Vadose Zone, the 95% confidence level was 0.99 mL/g which yielded a confidence window that was approximately one times the mean K_d of 1.49 mL/g, as is the case for most of the other isotopes. In the Lower Vadose Zone, the 95% confidence

level was 0.34 mL/g which yielded a window width of twice the mean K_d of 0.34 mL/g. The window is relatively larger than those identified for other isotopes. Finally, in the Aquifer Zone, the 95% confidence level was 4.87 mL/g which resulted in a window width of about 1.5 times the mean K_d of 6.97 mL/g.

The final radionuclide of concern in this study was ^{88}Y. The stratified data for this isotope did not reveal the common trend found for most of the other radionuclides. The compiled summary statistics for ^{88}Y are displayed in Table 9. The observed mean and median distribution coefficient values were relatively consistent across the different strata. The median K_d values were 1,673 mL/g, 1,503 mL/g, and 1,715 mL/g for the Upper Vadose, Lower Vadose, and Aquifer Zones respectively with similar values measured for the mean K_d. In both cases, the highest K_d values were again measured for the Aquifer Zone. That being said, however, the measured K_d values appear close enough that the differences between them seem relatively insignificant. Also all of these measured distribution coefficients fall within the expected range of 251 to 560,000 mL/g based on the literature review (Quinn et al., 2007).

Table 9. Stratified summary statistics for K_d compiled for ^{88}Y

Zone	Upper	Lower	Aquifer
Mean (mL/g)	1353	1526	1602
Standard Error (mL/g)	288	235	257
Median (mL/g)	1673	1503	1715
Standard Deviation (mL/g)	814	706	770
Minimum (mL/g)	173	539	328
Maximum (mL/g)	2197	3134	2747
Number of Samples	8	9	9
Confidence Level Mean (95.0%) (mL/g)	680	543	592

In terms of K_d variability, the Upper Vadose Zone displayed the highest degree of variability based on the measured standard deviation and variance. This is in contrast to most of the other isotopes which displayed the highest degree of variability in the Aquifer Zone. Following the Upper Vadose Zone, the Aquifer Zone displayed the next highest variability with the Lower Vadose Zone, as with the other isotopes, displaying the least amount of variability. Finally, the 95% confidence window for yttrium in the Upper Vadose Zone follows the same pattern as the previously discussed isotopes in that the 95% confidence level of 680 mL/g in this zone was again equivalent to a window with a width of about one times the mean K_d of 1,353 mL/g. The Lower Vadose and Aquifer Zones, however, displayed somewhat different trends compared to most of the other investigated isotopes. In the Lower Vadose Zone, the 95% confidence level was 543 mL/g which corresponded to a window equal to approximately 0.7 times the mean K_d of 1,526 mL/g. The Aquifer Zone displayed a similar trend in that the 95% confidence level for the mean was 592 mL/g which again yielded a confidence window of about 0.7 times the mean K_d of 1,602.

Some generalizations can be inferred from the above discussion. For the most part, isotopes in the Aquifer Zone tend to exhibit the highest degree of variability followed by the Upper Vadose Zone. Isotopes in the Lower Vadose Zone, in contrast, tend to exhibit the most consistency in K_d values. Isotopes in the Lower Vadose Zone also tend to display the lowest K_d values compared to those observed in the Upper Vadose and Aquifer Zones.

Finally, in general, the 95% confidence window for the mean tends to be approximately one times the mean K_d in the Upper Vadose Zone, 0.25 to 0.7 times the mean K_d in the Lower Vadose Zone, and two times the mean K_d in the Aquifer Zone for most isotopes.

4.3 CORRELATION ANALYSIS

Simple correlation coefficients were calculated between the K_d values and the soil parameters for the whole core and for the three stratified sub-surface zones (Table 10). Examination of Table 10 reveals that the correlation coefficients are not necessarily consistent when comparing the whole core correlations to the stratified correlations. Most notably, some of the expected K_d correlations with soil characteristics become more apparent in the stratified data. For example, greater positive correlations between the K_d values for ^{137}Cs and clay content were noted in the stratified sub-surface data than when the whole data set was placed together. Also, the expected increased levels of positive correlation were noted for the K_d values of $^{57,60}Co$ with soil pH. These levels were less apparent for the core as a whole.

Table 10. Correlation analysis for K_d and soil characterization parameters

Isotope	Soil Parameter	Whole Core	Upper Vadose Zone	Lower Vadose Zone	Aquifer Zone
^{109}Cd	CEC (meq/100g)	0.04	0.33	0.21	-0.16
	Soil pH	0.27	0.70	0.55	0.15
	Avg. Clay (%)	-0.21	-0.21	0.18	-0.18
	Al Content (ppm)	0.56	0.34	-0.04	0.60
	Ti Content (ppm)	0.83	0.63	-0.03	0.81
	Mn Content (ppm)	0.08	0.72	-0.06	0.28
	Fe Content (ppm)	0.65	0.61	0.34	0.84
^{137}Cs	CEC (meq/100g)	0.97	0.91	0.63	0.98
	Soil pH	-0.22	0.26	-0.22	-0.48
	Avg. Clay (%)	0.35	0.78	0.78	0.90
	Al Content (ppm)	0.62	0.95	-0.01	0.58
	Ti Content (ppm)	0.01	0.28	-0.41	-0.20
	Mn Content (ppm)	0.21	0.55	-0.20	0.77
	Fe Content (ppm)	0.36	0.80	-0.30	0.22
$^{57,60}Co$	CEC (meq/100g)	0.01	0.29	-0.31	-0.16
	Soil pH	0.28	0.70	0.88	0.19
	Avg. Clay (%)	-0.18	-0.10	-0.17	-0.17
	Al Content (ppm)	0.54	0.23	0.24	0.58
	Ti Content (ppm)	0.82	0.35	0.06	0.81
	Mn Content (ppm)	0.06	0.43	0.01	0.27
	Fe Content (ppm)	0.63	0.38	0.45	0.83
^{203}Hg	CEC (meq/100g)	0.30	0.36	0.71	0.24
	Soil pH	0.27	0.56	0.00	0.06
	Avg. Clay (%)	0.15	-0.03	0.51	0.12
	Al Content (ppm)	0.34	0.29	-0.10	0.30
	Ti Content (ppm)	0.31	0.66	0.21	0.30
	Mn Content (ppm)	0.29	0.36	-0.69	0.12
	Fe Content (ppm)	0.43	0.37	0.11	0.35
^{85}Sr	CEC (meq/100g)	0.83	0.95	0.05	0.85
	Soil pH	-0.21	0.59	0.47	-0.60
	Avg. Clay (%)	0.08	0.75	-0.03	0.77
	Al Content (ppm)	0.50	0.89	0.52	0.45
	Ti Content (ppm)	0.10	0.26	0.31	-0.25
	Mn Content (ppm)	0.06	0.45	-0.17	0.58
	Fe Content (ppm)	0.25	0.70	0.69	0.10
^{88}Y	CEC (meq/100g)	0.19	-0.55	-0.49	0.50
	Soil pH	-0.25	0.03	0.52	-0.72
	Avg. Clay (%)	-0.17	-0.46	-0.18	0.42
	Al Content (ppm)	0.00	-0.71	0.59	0.37
	Ti Content (ppm)	0.00	-0.32	0.07	0.01
	Mn Content (ppm)	-0.33	-0.55	0.16	0.17
	Fe Content (ppm)	-0.26	-0.66	0.46	0.21

4.4 DISTRIBUTION OF K_d VALUES

4.4.1 Whole Core Distributions

Log-probability plots of the whole core distributions are presented in Figure 4. Based on visual examination, the distributions for ^{109}Cd, ^{57}Co, ^{60}Co, ^{203}Hg, ^{85}Sr, ^{137}Cs, and ^{88}Y show relatively minor departures from linearity and could reasonably be described as log-normal. There were insufficient data for ^{241}Am and ^{139}Ce to make a judgment about the validity of a log-normal approximation. Also, it would be inappropriate to statistically describe these data sets because so many of the K_d values could not be adequately measured. Normal probability plots of the whole core data are presented in Appendix D. None of the plots are linear, indicating that the distributions can not be described as normal.

The results of the visual and Shapiro-Wilk statistical tests for normality (or log-normality) are presented in Table 11. The test statistics (W) for each radionuclide along with their associated p-values are listed in the table. The p-values indicate the confidence level at which the null hypothesis that the K_d values are normally (or log-normally) distributed can be rejected. For example, a p-value of 0.05 indicates that the null hypothesis can be rejected at the 95% confidence level. Based on the results of these tests, none of the isotopes could be approximated by normal or log-normal distributions except for ^{203}Hg which indicated log-normal distribution characteristics. However, it should be noted that the Shapiro-Wilk test is sensitive to even small deviations from normality, thus limiting its practical value in the context of scientific applications (Mendenhall and Sincich, 2003). In Table 11, if the sub-surface K_d values could not be characterized as either normally or log-normally distributed based on the Shapiro-Wilk test or based on visual inspection, then "Neither" is listed for the K_d characterization.

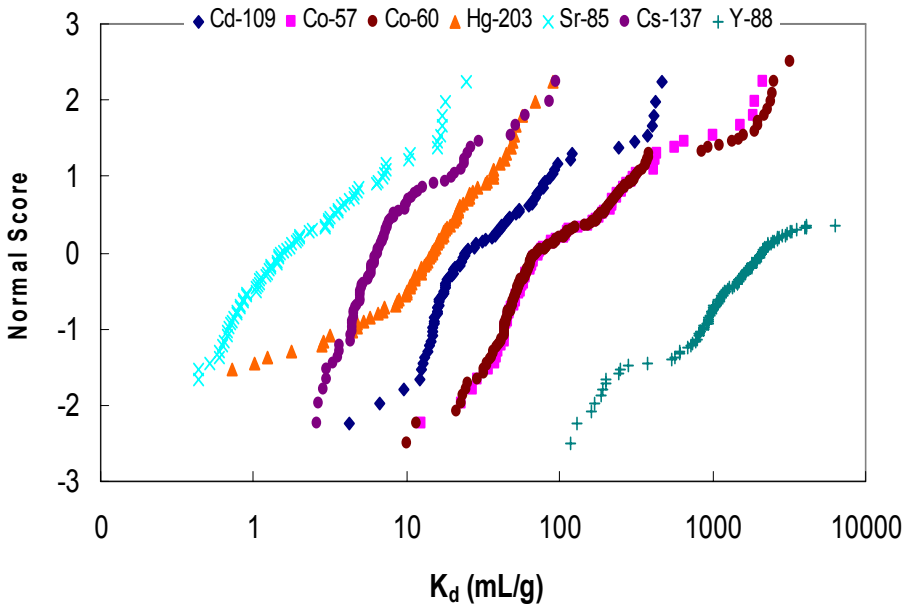

Figure 4. Log-probability plots of ^{109}Cd, ^{57}Co, ^{60}Co, ^{203}Hg, ^{85}Sr, ^{137}Cs and ^{88}Y. These isotopes can be approximated as log-normal distributions.

Table 11. Normality test results for the distribution characterization of K_d

	Normal		Log-Normal		Shapiro-Wilk	Visual
Isotope	W	p-value	W	p-value	K_d Distribution	K_d Distribution
^{109}Cd	0.30	<0.0001	0.90	<0.0001	Neither	Log-Normal
^{137}Cs	0.55	<0.0001	0.82	<0.0001	Neither	Log-Normal
$^{57,60}Co$	0.43	<0.0001	0.92	<0.0001	Neither	Log-Normal
^{203}Hg	0.95	0.0007	0.99	0.5371	Log-Normal	Log-Normal
^{85}Sr	0.66	<0.0001	0.94	0.0008	Neither	Log-Normal
^{88}Y	0.88	<0.0001	0.96	0.0022	Neither	Log-Normal

4.4.2 atified Core Distributions

Distributions like those generated for the core as a whole were also developed for each of the sub-surface strata. These probability and log-probability plots can be viewed in Figure 5 through Figure 10. apiro-Wilk tests were also completed for the stratified distributions. A summary of these results is listed in Table 12.

Based on visual inspection, in the Upper Vadose Zone, ^{109}Cd, $^{57,60}Co$, and ^{88}Y, the isotopes with the highest relative K_d values of the radionuclides included, displayed an apparent normal distribution while ^{85}Sr could be approximated by a log-normal distribution. Cesium and mercury could not be approximated by either distribution type. Examining the Lower Vadose Zone, the K_d values for all of the isotopes could be approximated by a normal distribution. Finally, in the Aquifer Zone, ^{88}Y displayed apparent normal distribution characteristics for K_d while ^{109}Cd and ^{85}Sr could be approximated with a log-normal distribution. The remaining isotopes, ^{203}Hg, ^{137}Cs, and $^{57,60}Co$, deviated greatly from linearity in both the probability and log-probability plots and, thus, could not be characterized by either distribution.

The results of the Shapiro-Wilk tests confirm many of the visual approximations described above. However, there were a few cases of disagreement between the visual approximation and the statistical test. These differences can be attributed to the subjective nature of the visual approximation and to the relatively high sensitivity of the Shapiro-Wilk test to only small deviations from normality.

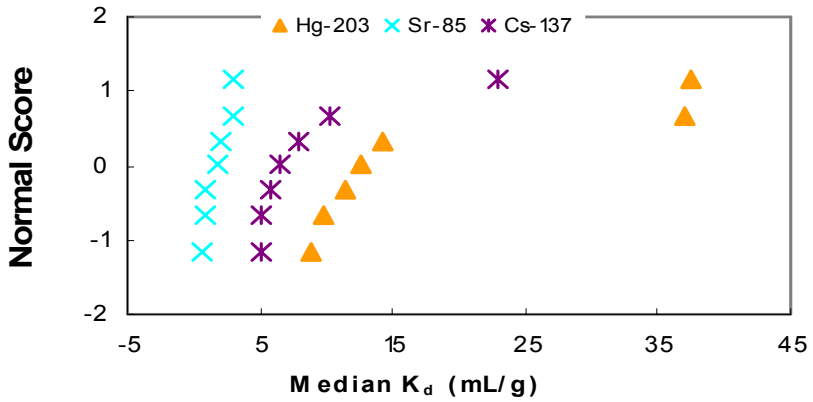

(a)

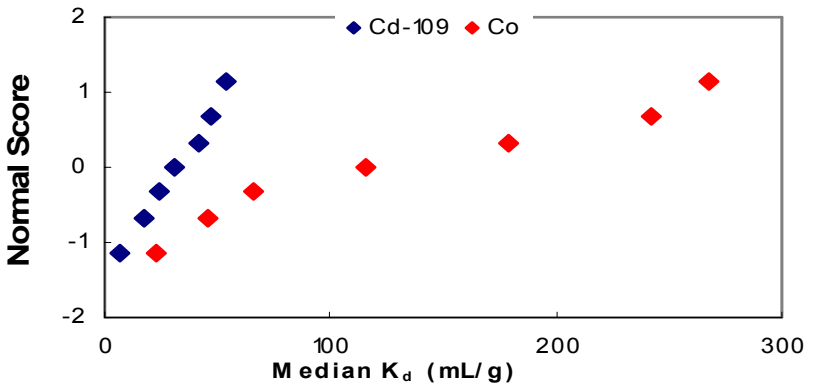

(b)

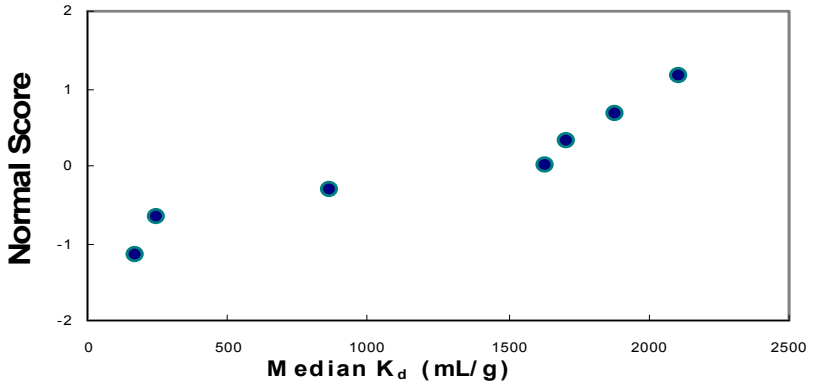

(c)

Figure 5. Normal probability plots for Kd of: a) ^{203}Hg, ^{85}Sr, and ^{137}Cs; b) ^{109}Cd and Co; and c) ^{88}Y in the Upper Vadose Zone

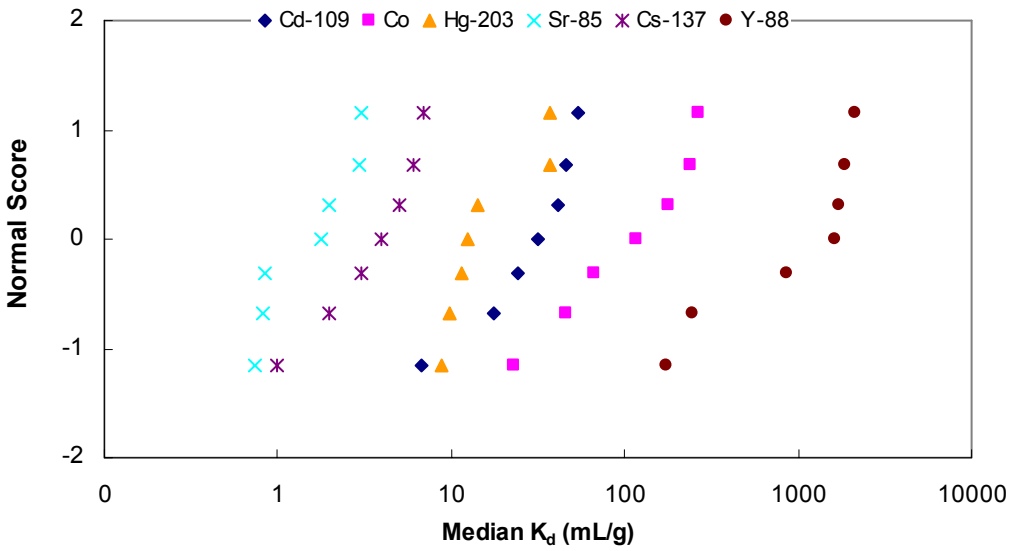

Figure 6. Log-probability plot for K_d of the radionuclides in the Upper Vadose Zone

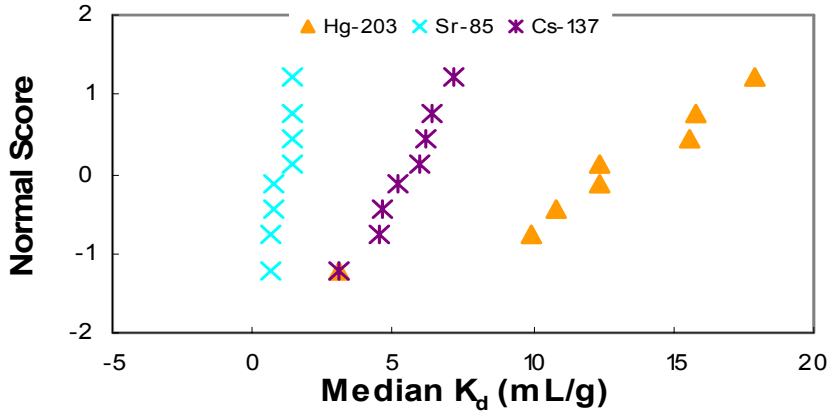

(a)

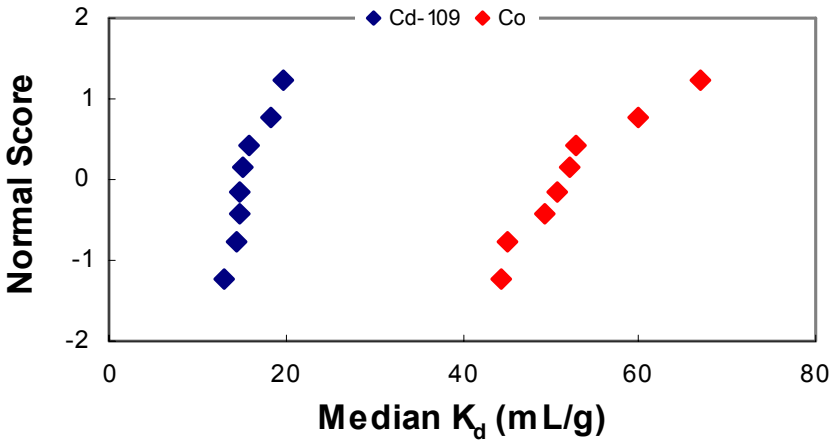

(b)

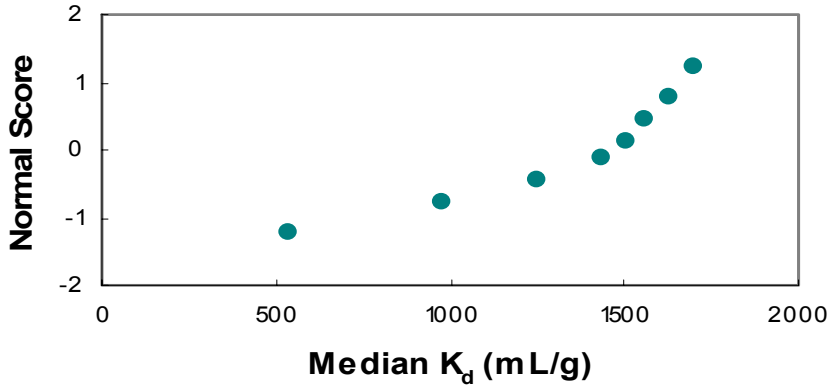

(c)

Figure 7. Probability plots for K_d of: a) ^{203}Hg, ^{85}Sr, and ^{137}Cs; b) ^{109}Cd and Co; and c) ^{88}Y in the Lower Vadose Zone

.

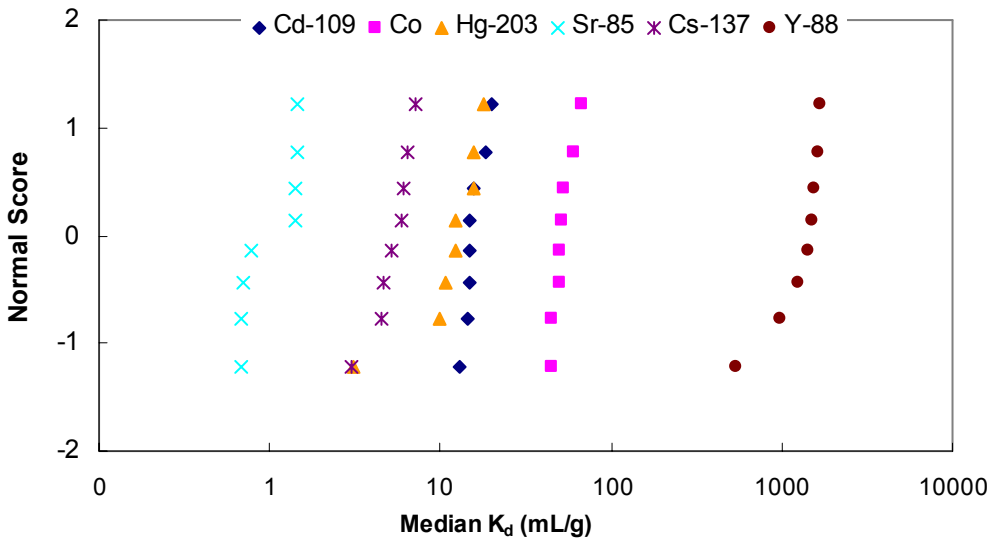

Figure 8. Log-probability plot for K_d of the radioisotopes in the Lower Vadose Zone

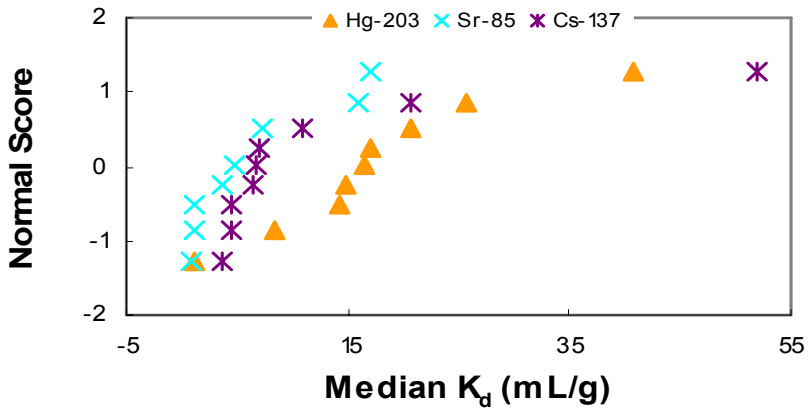

(a)

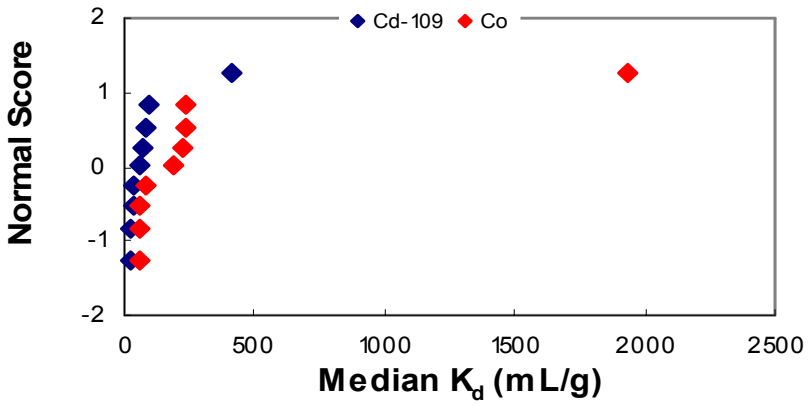

(b)

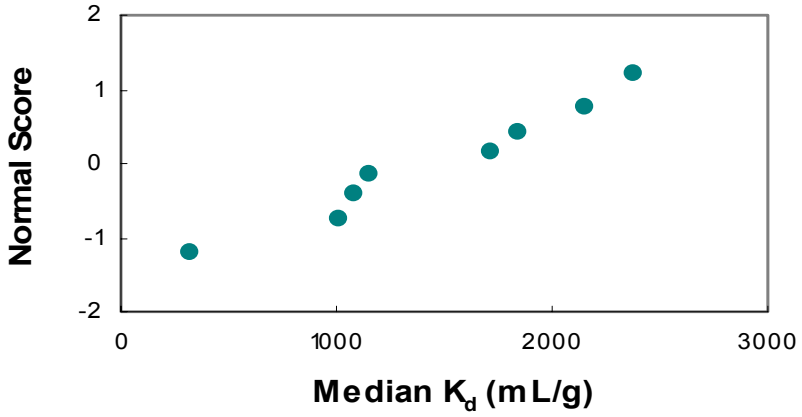

(c)

Figure 9. Probability plots for K_d of: a) ^{203}Hg, ^{85}Sr, and ^{137}Cs; b) ^{109}Cd and Co; and c) ^{88}Y in the Aquifer Zone

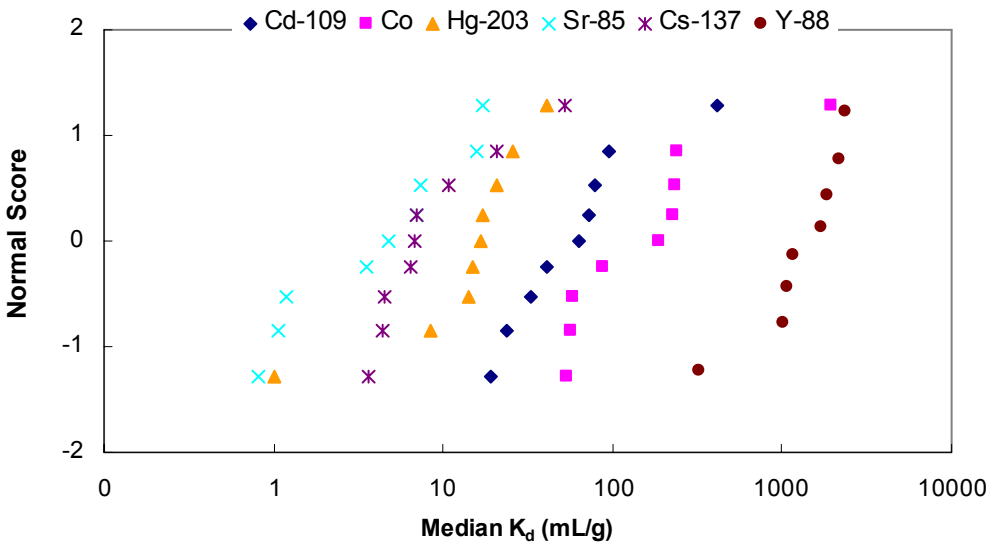

Figure 10. Log-probability plot for K_d of the radioisotopes in the Aquifer Zone

Table 12. Summary of stratified K_d value distributions for the Upper Vadose, Lower Vadose, and Aquifer Zones

		Normal		Log-Normal		Shapiro-Wilk	Visual
Isotope	Strata[(a)]	W	p-value	W	p-value	K_d Distribution	K_d Distribution
^{109}Cd	UVZ	0.98	0.9536	0.94	0.5930	Normal	Normal
	LVZ	0.88	0.1446	0.94	0.6147	Log-Normal	Normal
	AZ	0.69	0.0010	0.91	0.2858	Log-Normal	Log-Normal
^{137}Cs	UVZ	0.75	0.0075	0.84	0.0729	Neither	Neither
	LVZ	0.89	0.1954	0.9	0.3473	Normal/Log-Normal	Normal
	AZ	0.64	0.0003	0.86	0.1067	Neither	Neither
$^{57,60}Co$	UVZ	0.91	0.3810	0.91	0.3407	Normal/Log-Normal	Normal
	LVZ	0.90	0.2565	0.93	0.5361	Normal/Log-Normal	Normal
	AZ	0.63	0.0002	0.84	0.0626	Neither	Neither
^{203}Hg	UVZ	0.8	0.0267	0.84	0.0838	Neither	Neither
	LVZ	0.97	0.8659	0.85	0.1174	Normal	Normal
	AZ	0.93	0.5153	0.83	0.0472	Normal	Neither
^{85}Sr	UVZ	0.84	0.0766	0.83	0.0638	Neither	Log-Normal
	LVZ	0.80	0.0220	0.78	0.0128	Neither	Normal
	AZ	0.85	0.0665	0.92	0.3790	Log-Normal	Log-Normal
^{88}Y	UVZ	0.86	0.1240	0.77	0.0148	Neither	Normal
	LVZ	0.86	0.0893	0.64	0.0009	Neither	Normal
	AZ	0.96	0.7918	0.78	0.0127	Normal	Normal

[(a)] UVZ = Upper Vadose Zone; LVZ = Lower Vadose Zone; AZ = Aquifer Zone.

A summary of the statistical regression models developed for each isotope is presented in Table 13. These models are in the form of first- and second-order regressions as shown below:

$$K_d(mL/g) = \beta_0 + \beta_1 x_1 + \beta_2 x_2 + \ldots + \beta_6 x_1^{\,2} + \beta_7 x_2^{\,2} + \ldots + \beta_{10} x_5^{\,2},$$

where β_0 is the y-intercept of the regression model and the remaining β values represent the coefficients for each of the model variables. If a variable is not included in the regression model for a given isotope, then the corresponding β parameter will be zero.

Table 13. Variables and corresponding parameters for statistical regression models of K_d for radionuclides

Radio-nuclide	^{109}Cd	^{137}Cs	^{57}Co	^{60}Co	^{203}Hg	^{85}Sr
Intercept	-171.97	16.24	-655.83	-763.41	-79.56	-1.66413
$CEC_{(meq/100g)}$	0	-1.26	0	0	22.63	1.95302
Clay(%)	0	0.00451	0	0	0	0
$Al_{(ppm)}$	0.19566	-0.1673	1.10	1.09	0.09377	0
$Fe_{(ppm)}$	0.06076	0	0.10029	0.17918	0	0
$Ti_{(ppm)}$	11.12	0	-7.79	14.33	0.86682	0
CEC^2	0	1.07	0	0	-1.56205	0
$Clay(\%)^2$	0	0.00409	0	0	0	0
Al_3^2	-0.000136	0.00000615	-0.0004556	-0.000553	-0.000036	0
Fe^2	-0.000002	0	-0.0000029	-0.0000054	0	0
Ti^2	0.01651	0	0.79212	0.59082	0.00757	0
Adjusted R^2	0.5600	0.9873	0.8654	0.7117	0.4958	0.6430
Global F p-value	0.0006	<0.0001	<0.0001	<0.0001	0.0021	<0.0001
C(p)	5.0025	8.4039	5.1204	5.0300	6.0663	-1.1751

Examination of the models and the measures of adequacy, particularly the adjusted R^2 values, indicated that, while all six models offered some degree of significant information regarding the variation in K_d, only the models for cesium and cobalt exhibited a reasonable fit to the data. For example, the adjusted R^2 values for cadmium, mercury, and strontium were 0.56, 0.55, and 0.61 respectively. This indicates that the models can explain only about 55 to 61% of the variation in K_d. This degree of correlation is generally unacceptable. models may, however, be useful for a first approximation. Conversely, the adjusted R^2 values for ^{137}Cs, ^{57}Co, and ^{60}Co are 0.9879, 0.8645, and 0.7117 respectively. As with the other isotopes, these values indicate that the models can account for about 99, 86, and 71% of the variation in K_d for cesium and the two cobalt isotopes. Generally, these percentages are much more acceptable for a practical and useable model than those that were generated for cadmium, mercury, and strontium.

Most of the factors that were expected to show high correlation with K_d were included in the final model. The literature review notes that cadmium is expected to be affected by complexation with aluminum and iron oxides. As shown in Table 13, both aluminum and iron content were significant factors in the final statistical model. Somewhat surprisingly, however, in addition to these variables, titanium was also found to be a significant factor, and possibly the most significant factor based on the relative magnitudes of the β parameters, for cadmium sorption. It was anticipated that the presence of complexing ions and soil pH would be controlling factors for cobalt sorption. While the observed significance of aluminum, iron, and titanium content confirmed the dependence on complexing ions, soil pH was not found to be significant. This observation is likely a result of the fact that only small variations in soil pH were observed among the 27 different soil samples from the BGO-3A core. Finally, as expected for strontium, CEC was shown to be the most significant factor for modeling strontium sorption.

5.0 CONCLUSIONS

The 95-percentile range and type of distributions assigned to radionuclide K_d values should be assigned based on the following general rules. These general rules are derived from the measurements described in this report, some geochemical/geological consideration, and parsimony.

- The 95% confidence level for the mean K_d was twice the mean in the Aquifer Zone, equal to the mean for the Upper Vadose Zone, and half the mean for the Lower Vadose Zone.
- The distribution of K_d values was log normal in the Upper Vadose Zone and Aquifer Zone, and normal in the Lower Vadose Zone.

Preliminary reports that did not have site-specific data and written with the expressed purpose to provide early guidance for data input to Monte Carlo simulations generally had appreciably greater 95% confidence ranges (Kaplan and Millings 2006, Shine 2007). This is the first report of radionuclide K_d variability in the literature. This data supports the assignment of unique ranges and distributions of radionuclide K_d values by hydrostratigraphic unit. Perhaps more importantly, it supports the use of more narrow ranges of K_d values (0.5x, 1x, & 2x the mean) compared to using the distributions measured in the entire subsurface region of interest (1 to 2 orders of magnitude of the mean). Using ranges and distribution coefficients that are specific to the hydrostratigraphic unit will improve model accuracy and reduces model uncertainty.

6.0 ACKNOWLEDGEMENTS

This report was taken from Mr. Kelly Grogan's thesis.[3] Additional text not found in Mr. Grogan's thesis was added to this report to make the findings more applicable to SRS programmatic needs. Conversely, portions of his thesis not relevant to the subject matter of this report were omitted. Funding for this work came from the U.S. Department of Energy Nuclear Engineering and Health Physics Fellowship Program sponsored by the U.S. Department of Energy's Office of Nuclear Energy, Science, and Technology; and Site Regulatory Integration and Planning Division (SRIP, formally Solid Waste) of the SRS.

7.0 REFERENCES

Ames, L. L., and Rai, D. 1978. *Radionuclide Interactions with Soil and Rock Media: Volume I: Processes Influencing Radionuclide Mobility and Retention, Element Chemistry and Geochemistry, Conclusions and Evaluation*. EPA, 520/6-78-007-A. U. S. EPA, Washington DC.

Bradbury, M. H., and F. A. Sarott. 1995. *Sorption Databases for the Cementitious Near-field of a L/ILW Repository for Performance Assessment.* PSI Bericht Nr. 95-06. Paul Scherrer Institut, Villigen, Switzerland.

Cantrell, K.J., Serne, R.J., and Last, G.V. 2003, June. *Hanford Contaminant Distribution Coefficient Database and Users Guide*. PNNL-13895 Rev.1 Pacific Northwest National Laboratory, Richland, WA

[EPA] Environmental Protection Agency 2001, Dec. *Risk Assessment Guidance for Superfund: Vol III, Pt A, Process for Conducting Probabilistic Risk Assessment*. U.S. EPA 540-R-02-002, OSWER 9285.7-45, PB2002-963302. U.S. EPA, Washington, DC

Fjeld, R. A., Eisenberg, N. A., and Compton, K. L. 2007. *Quantitative Environmental Risk Analysis for Human Health*. John Wiley & Sons, Inc. 284-289.

Grogan, K. 2008. *Spatial Variability of Radionuclide Distribution Coefficients at the Savannah River Site and the Subsurface Transport Implications.* M.S. Thesis. Clemson University, Clemson, SC.

Kaplan D. I. and Millings, M. R. 2006. *Early Guidance for Assigning Distribution Parameters to Geochemical Input Terms to Stochastic Transport Models.* WSRC-STI-2006-00019. Washington Savannah River Company, Aiken, SC.

Kaplan, D. I. 2006. *Geochemical Data Package for Performance Assessment Calculations Related to the Savannah River Site.* WSRC-TR-2006-00004, Rev. 0. Washington Savannah River Company, Aiken, SC.

[3] Grogan, K. 2008. Spatial Variability of Radionuclide Distribution Coefficients at the Savannah River Site and the Subsurface Transport Implications. M.S. Thesis. Clemson University, Clemson, SC.

Kaplan, D. I., K. E. Parker, and I. Kutnyakov. 1998. *Radionuclide Distribution Coefficients of Sediments Collected from Borehole 299-E17-21*. PNNL-11966. Pacific Northwest National Laboratory, Richland, WA.

Krupka, K. M., D. I. Kaplan, G. Whelan, R. J. Serne, and S. V. Mattigod. 1999a. Understanding Variation in Partition Coefficient, Kd, Values. Volume 1: The Kd Model, Methods of Measurement, and Application of Chemical Reaction Codes. EPA 402-R-99-004A. Office of Air and Radiation, Office of Solid Waste and Emergency Response, U.S. Environmental Protection Agency, Washington, DC. (http://www.epa.gov/radiation/cleanup/partition.htm)

Krupka, K. M., D. I. Kaplan, G. Whelan, R. J. Serne, and S. V. Mattigod. 1999b. Understanding Variation in Partition Coefficient, Kd, Values. Volume II: Review of Geochemistry and Available Kd Values, for Cadmium, Cesium, Chromium, Lead, Plutonium, Radon, Strontium, Thorium, Tritium (3H), and Uranium. EPA 402-R-99-004A. Office of Air and Radiation, Office of Solid Waste and Emergency Response, U.S. Environmental Protection Agency, Washington, DC.

Krupka, K. M., R. J. Serne, and D. I. Kaplan. 2004. *Geochemical Data Package for the 2005 Hanford Integrated Disposal Facility Performance Assessment.* PNNL-13037, Rev. 2, Pacific Northwest National Laboratory, Richland, WA.

Lee, S.-Z., Chang, L., Chen, C.-M., Tsai, Y.I., and Liu, M.-C. 2001. Predicting Soil-Water Partition Coefficients for Hg(II) from Soil Properties. *Water Sci. Technol.* 43:2:187-196.

Mendenhall, William and Sincich, Terry. 2003. *A Second Course in Statistics: Regression Analysis*. Pearson Education, Inc. 634.

Meyer, P.D., Rockhold, M.L., and Gee, G.W. 1997. *Uncertainty Analyses of Infiltration and Subsurface Flow and Transport for SDMP Sites.* NUREG/CR-6565. U.S. NRC, Washington, D.C.

Quinn, K., Byrne, R., and Schijf, J. 2007. Sorption of Yttrium and Rare Earth Elements by Amorphous Ferric Hydroxide: Influence of Temperature. *Environ. Sci. Technol.* 41: 541-546.

Shine, E. P. Inter-Office Memorandum SRNL-SCS-2007-00011, Rev. 1.0. Washington Savannah River Company, Aiken, SC

Walpole, R. E., and Myers, R. H.. 1978. *Probability and Statistics for Engineers and Scientists, 2nd ed*. Macmillan Publishing, New York, New York, 580 p.

Wieland, E., and Van Loon, L. R. 2003. *Cementitious Near-Field Sorption Data Base for Performance Assessment of an ILW Repository in Opalinus Clay.* PSI Bericht 03-06, Paul Scherrer Institut, Villigen, Switzerland.

8.0 APPENDIX A: DETAILED DESCRIPTION OF SAMPLE COLLECTION, SEDIMENT CHARACTERIZATION PROCEDURES, DISTRIBUTION COEFFICIENT PROCEDURE, AND SIMPLE AND MULTIPLE REGRESSION ANALYSES

8.1 SAMPLE COLLECTION

Thirty-two soil samples were obtained from the E-Area of the Savannah River Site. The E-Area is located in the central northern portion of the Savannah River Site and contains several burial trenches. Figure A.1 presents a map of SRS showing the relative position of E-Area at SRS. All but one of the soil samples were obtained from cores. Figure A.2 shows the location of each core.

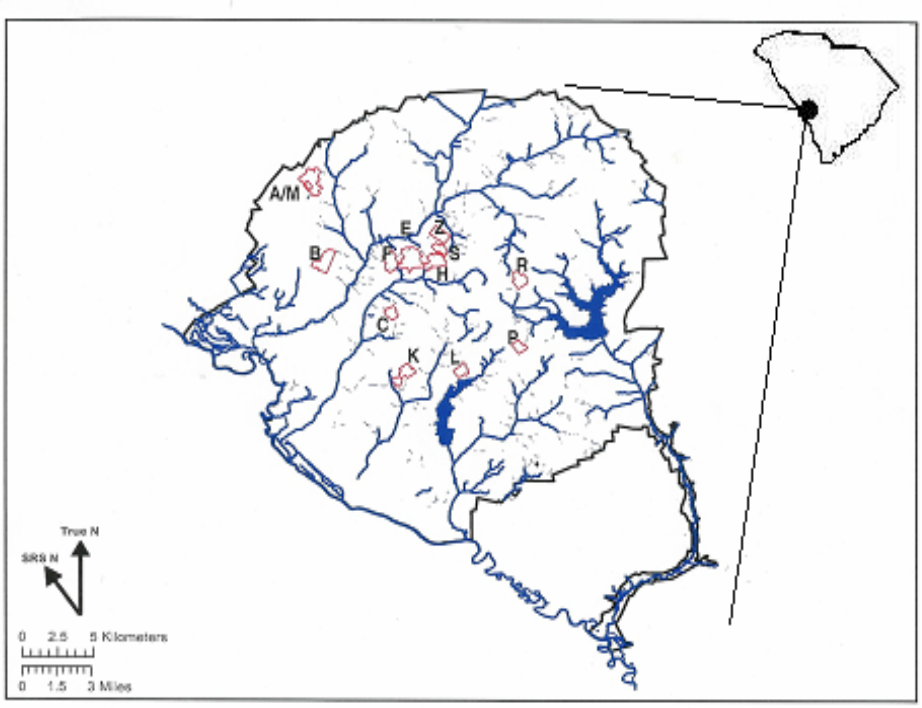

Figure A.1. Relative position of the E-Area burial grounds at SRS

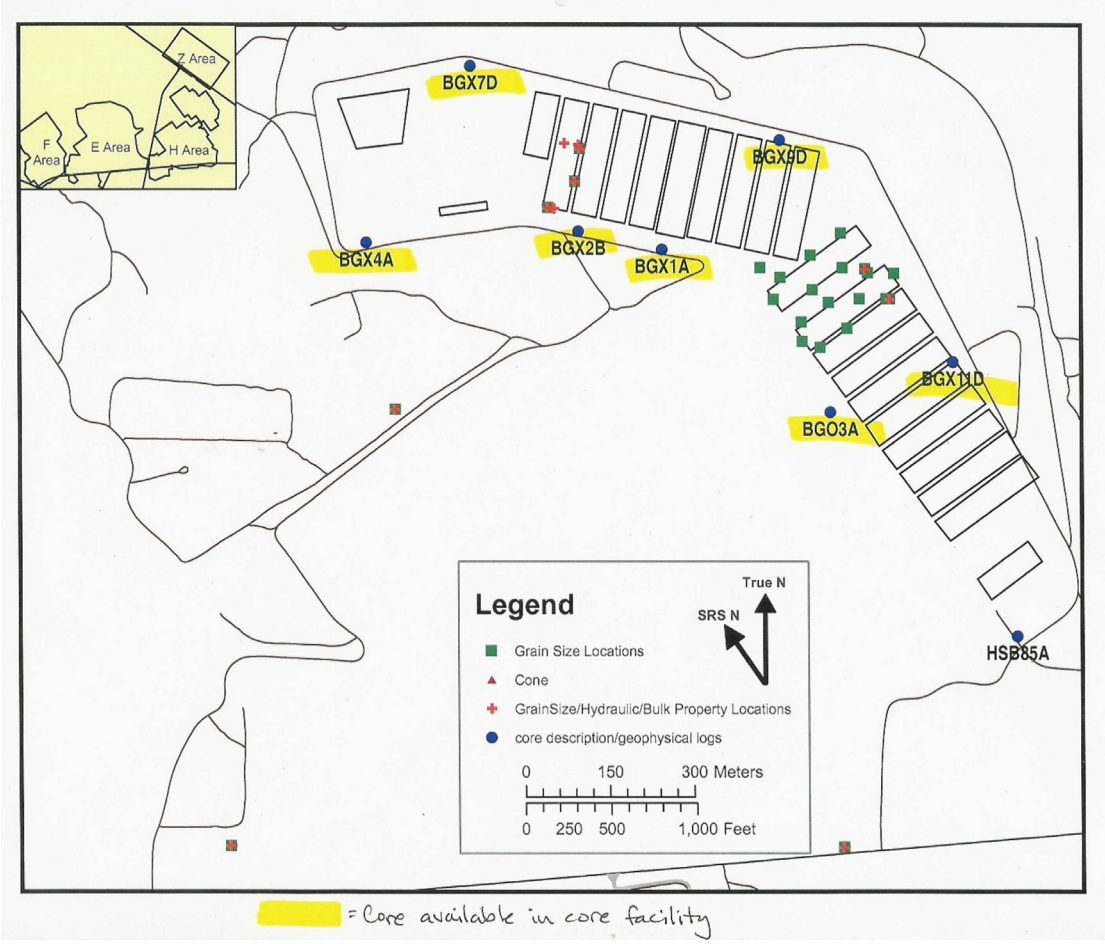

Figure A.2. Bore hole locations within the E-Area burial grounds

Of the thirty-two samples, twenty-seven were collected from a single core, BGO-3A. The BGO-3A core was located in an uncontaminated section of E-Area near the burial trenches on the eastern side of the burial grounds. Three samples were collected from the BGX-2B core and one sample was taken from the BGX-11D core. The BGX-2B core [illegible]e from an uncontaminated area in the northern portion of E-Area near other burial trenches while the BGX-11D core is located adjacent to the BGO-3A core and was also uncontaminated. These core samples were included for their characteristic tan clay confining zone layers. A final lysimeter control soil sample was collected for a total of thirty-two soil samples. This latter sample was included because it has been extensively characterized and is treated on the Savannah River Site as the typical "clayey sediment" in risk calculations. All of these core samples were collected from depths ranging from 11 to 100 ft beneath the surface. For the BGO-3A core, samples were collected each 2.5 to 5 ft. For the BGX-2B core, samples were collected from 78.5, 80, and 85 ft below the surface. For the BGX-11D core, the sample was taken from 96 ft below the surface. Each sample was approximately two kg in weight and was stored in plastic ziplock bags for transport. The samples were approximately 15 cm in length with a 15 cm diameter. Prior to sample preparation, each soil sample was stored in its own ziplock bag at ambient temperature. Two important assumptions were made during this sampling process. First, the BGO-3A core was assumed

to be representative of the entire E-Area. Second, it was assumed that the soil lenses present in the E-Area soil are uniform across the E-Area.

8.1.1 Sample Preparation

Each soil sample was air dried under a fume hood at ambient temperature. Once dry, as determined by visual observation, each sample was photographed for visual record. Photographs of representative soil samples are presented in Figure A.3. The soil samples were then sieved using a 2-mm sieve to remove large rocks and debris from the soils. After sieving, the remaining soil for each sample was again stored in its own ziplock bag under ambient conditions until ready for use.

Figure A.3. Photographs of representative soil samples from the BGO-3A core

8.1.2 Sample Pre-equilibration

Each soil sample was pre-equilibrated with natural ground water taken from a well at the Savannah River Site. Pre-equilibration was accomplished by collecting 1.00 g of each soil sample in a labeled 50 mL polypropylene Falcon centrifuge tube. A 20 mL volumetric pipette was then used to add 40 mL of the SRS ground water to each sediment in the centrifuge tubes. The centrifuge tubes were then capped and placed on a shaker at a low setting for a period of three days. After this period, the samples were centrifuged at 2660 rpm for 20 minutes to separate the sediment and ground water. The ground water was then decanted and replaced with 10 mL of fresh SRS ground water using a 10 mL volumetric pipette. The tubes were again capped and placed on a shaker for a period of one day. After one day, the samples were again centrifuged at 2660 rpm for 20 minutes and the ground water decanted. One final SRS ground water wash of 10 mL was then added to each sample. The centrifuge tubes were capped and placed on a shaker for approximately one hour. After this one hour period the sample was once more centrifuged at 2660 rpm for 20 minutes and the ground water decanted from the sediment. At this point the sample sediment was considered to be pre-equilibrated. This method was developed based on previous K_d batch experiments completed by Krupka et al. (1999). Confirmation of pre-equilibration was provided through pH measurements of the decanted ground water washes indicating stable and neutral pH levels in the wash effluent. Pre-equilibration and subsequent spike procedures were completed in sets of five sediment samples at a time.

8.1.3 Spike Addition

After pre-equilibration, the sediment samples were spiked using a solution of SRS ground water and a mixed-gamma standard containing ^{241}Am, ^{109}Cd, ^{139}Ce, ^{57}Co, ^{60}Co, ^{203}Hg, ^{113}Sn, ^{137}Cs, ^{85}Sr, and ^{88}Y purchased from Analytics Inc. The spike solution was prepared in a batch-wise fashion. To begin preparation of the spike solution, 150 mL of SRS ground water was added to a 500 mL Teflon beaker. A 1 mL volumetric pipette was then used to add 2 mL of the mixed-gamma standard to the beaker. The pH of the spike solution was then measured using a pH electrode. Solutions of various concentrations of HCl and NH_4OH were then used to neutralize the spike solution to approximately pH 7. Once neutralized, the spike solution was diluted to 225 mL with SRS ground water as determined by weight. The final spike solution pH was then measured and recorded. Because of the relatively short half-life of ^{85}Sr an additional ^{85}Sr spike was necessary for each batch of spike solution after the first. This additional spike was obtained from a stock solution of ^{85}Sr containing 2.71 µCi/mL. A [illegible] mL aliquot of this solution was collected in a glass container and diluted to 50 mL with 1.5 M HCl solution. [illegible] mL of the resulting solution were then added to each batch of the mixed-gamma standard spike solution prior to neutralization after the first batch.

After preparation of the spike solution, volumetric pipettes were used to add 45 mL of the spike solution to each of five pre-equilibrated sediment samples in the labeled centrifuge tubes. The centrifuge tubes were then capped and placed on the same shaker used for pre-equilibration and allowed to shake at a low setting for seven days to obtain equilibrium (Krupka et al., 1999b). Based on the initial activity of the mixed-gamma standard, each centrifuge tube contained an activity of approximately 888 Bq ([illegible]24 µCi). After this contact time the sediment solutions were centrifuged for 20 minutes at 2,660 rpm. The aqueous phase of each sample was then transferred to a separate and correspondingly labeled

centrifuge tube using 5 mL disposable pipettes. All centrifuge tubes were then capped and stored at ambient conditions for later analysis.

8.1.4 Sample Analysis

For analysis, two different HPGe gamma detectors were used to count the solid and aqueous phases. A sample positioning apparatus was designed to maintain the position and geometry of the centrifuge tubes within the HPGe detectors during counting. Each solid and aqueous phase was counted for 24 hours. The results of counting were then compiled by the Genie 2K program and peak areas and energy levels were recorded. Similar batch experiments have been conducted by Krupka et al. (1999b) with the notable exception that, in this study, concentrations were measured in both the solid and aqueous phases (1999). In previous studies, determination of K_d values was accomplished based on the change in the aqueous phase concentration of the radionuclide and solid phase measurements were not made (Krupka et al. 1999b).

From the data obtained from the gamma-ray measurements, the K_d value for each radionuclide present in the standard was determined based on the measured concentrations of the radionuclides in each phase, after correction for background. It should be noted that the measured concentration in the solid phase includes precipitation as well as sorption. Background counts for each phase were determined by preparing a background sample for both the solid and aqueous phases. The solid phase background was prepared by adding 1 g of a known low background sand to a 50 mL polypropylene Falcon centrifuge tube. One milliliter of the SRS ground water was then added to the sand in the centrifuge tube to account for the moisture that was present in the solid phases of experimental samples. The aqueous phase background was prepared by adding 40 mL of the SRS groundwater to a centrifuge tube. These background samples were then counted for 24 hours using the previously described set-up for the HPGe detectors. Efficiency calibration standards were also prepared to calibrate the detectors and the Genie 2K system. The solid phase calibration standard consisted of 1 g of the low-background sand in a 50 mL centrifuge tube. To this was added a very small (< 1 mL) amount of SRS ground water and 1 mL of the undiluted mixed-gamma standard. The aqueous phase calibration standard consisted of 39 mL of SRS ground water in a 50 mL Falcon centrifuge tube along with 1 mL of the undiluted mixed-gamma standard. These standards were counted for 3 hours on the HPGe detectors periodically to maintain proper calibration of the detection system. Finally, a blank sample was also prepared by adding 45 mL of the neutralized spike solution to a 50 mL Falcon tube without allowing it to contact any sediment. This sample was counted for three hours.

Three trials were completed for each soil sample and summary statistics were then compiled for uncertainty and variability analysis. Characterization of K_d distributions was completed by graphing the resulting data in Microsoft Excel.

8.2 SOIL CHARACTERIZATION

Another major task for this study was the characterization of the soil samples collected from the E-Area as well as the lysimeter control sediment. This characterization included determination of clay fraction, iron oxide content, general iron, titanium, and manganese content, as well as cation exchange capacity and soil pH. Soil characterization was completed with the help of Dr. John Seaman of the Savannah River Ecology Laboratory (SREL) and the Clemson University Agricultural Extension Service.

8.2.1 Clay Fraction Determination

The clay fraction for each sediment sample was determined using the micropipette method developed by Miller and Miller (1987) and Burt et al. (1993). To begin the analysis, each sediment sample was passed through a 2 mm screen. Four grams of each sediment was then treated with 10 mL of water and 10 mL of a dispersing agent (5 g/L sodium hexametaphosphate) in a 50 mL centrifuge tube. The mixture was then placed on a shaker and mixed for 2 hours. After this time, 20 mL of water was added to each sample, and the solutions were shaken by hand to ensure that all soil particles were in solution. The solutions were then placed in a rack and allowed to settle for approximately 1 hour and 50 minutes. After settling a micropipette was used to remove 5 mL of the suspension from the middle of the tube. This 5 mL aliquot was then injected into a pre-weighed aluminum pan. Finally, the aliquot was oven-dried and weighed to determine clay content. Two trials were completed for each of the samples form the BGO-3A core and for the lysimeter control sediment. No trials were completed for any of the sediments from BGX-2B or BGX-11D due to sample scarcity.

8.2.2 Iron Oxide Extraction and Analysis

The iron oxide content of each of the soil samples was determined using the extraction method developed by Kunze (1986) and Mehra (1960). To begin, 5 g of each soil were measured into labeled 50 mL centrifuge tubes. Twenty-five mL of CDB solution (0.27 M sodium-citrate dihydrate/0.11 M sodium bicarbonate) was then added to each tube. The sediment suspensions were then heated in a water bath at 80^{o}C. Once heated, 0.75 g of sodium dithionite was added to each solution and stirred continuously for approximately 1 minute. Each suspension was then stirred intermittently for the next 15 minutes under a fume hood. The tubes were then balanced with CDB solution and centrifuged at 10,000 rpm for 15 minutes. After centrifugation the supernatant was decanted into a labeled 100 mL volumetric flask. The remaining solid was then washed with 25 mL of CDB solution, shaken, centrifuged, and decanted into the appropriate volumetric flask in order to remove any residual iron. This wash was then repeated one final time. After combining the extracts, CDB solution was used to dilute the extraction volume in the flask to 100 mL. An aliquot of this dilution was then acidified with 10% HNO_3 and analyzed with ICP-MS. Three trials were completed for each soil sample.

8.2.3 Clay Mineralogy Analysis

Soil samples from six different depths (17.5 ft, 42 ft, 80 ft, 90 ft, 95 ft and 100 ft) were selected for clay mineralogy analysis. To begin, 25 g of each soil was collected in six centrifuge bottles. To each bottle was added 150 mL of 0.025 M Na_2CO_3 solution to raise the pH to approximately 9.5. These solutions were then placed on a shaker and allowed to shake overnight in order to disperse the soils. The next morning the dispersions were removed from the shaker and centrifuged at 1000 rpm for 2 minutes. The supernatant from each centrifuge bottle was then decanted into its own corresponding labeled 2 L bottle. Deionized water was then added to each of the centrifuge bottles up to the 10-cm mark, and the bottles were placed on the shaker for another 15 minutes. After this time, the centrifuge bottles were removed from the shaker and centrifuged again for 2 minutes at 1000 rpm. The supernatant was then decanted into the same labeled 2 L bottles. This process was repeated until the supernatant from the centrifuge bottles ran clear. Once all of the centrifuge bottle

supernatants ran clear, sufficient NaCl was added to each of the 2 L bottles so that the final NaCl concentration was approximately 1 M. This step served to promote flocculation of the clay sediment. The 2 L bottles were shaken to dissolve the NaCl and then allowed to settle overnight. After settling overnight, the clear supernatant was siphoned out of the 2 L bottles and discarded (Whittig and Allardice, 1986).

After extracting the clay sediments a volume equivalent to approximately 200 mg of clay was pipetted into each of two new centrifuge tubes. Two tubes were designated for each sediment depth; one labeled "K-saturated" and the other labeled "Mg-saturated." After each clay sediment was added to its corresponding centrifuge tubes, 30 mL of 1 M KCl solution was added to the "K-saturated" tubes and 30 mL of 0.5 M $MgCl_2$ solution was added to the "Mg-saturated tubes." The tubes were then placed on a shaker for 15 minutes to equilibrate after which time the tubes were centrifuged for 5 minutes at 5000 rpm. The clear supernatant from each tube was discarded, and the process was repeated three more times. After discarding the rinse solution for the fourth time, the tubes were filled with DI water up to the 30 mL mark and placed on a shaker once again in order to break up any aggregates that may have formed.

While the DI water suspension was equilibrating, the Drever method was used to create three XRD slides for each clay sediment (Drever, 1973). As part of this process, an Erlenmeyer filtration apparatus was setup using a 25 mm polycarbonate filter. The clay sediments were removed from the shaker and filtered using the filtering apparatus. After filtering the DI water, excess 1 M KCl or 0.5 M $MgCl_2$ (depending on the saturation label) saturating solution was filtered through the clay. Finally, another aliquot of DI water was filtered through the clay. Once the water was finished filtering, the polycarbonate filter was removed leaving a uniform clay layer on its surface. A glass slide was placed on top of the clay on the filter and pressed so as to transfer a thin and uniform layer of clay to the slide. These slides were then used for XRD analysis. The slide treatments consisted of Mg saturation, Mg and glycerol saturation, and K saturation. The K-saturated slides were heat treated at 110, 300 and 550 °C prior to x-ray analysis. Mineralogy from XRD analysis was determined based on standardized criteria (Brindley and Brown 1980; Jackson 1979; whittig and Allardice 1986).

Excess clay from the Mg-saturated slides was dried and retained for thermal gravimetric analysis (TGA). Approximately 10 mg of each of the Mg-saturated sediments was added to a platinum pan and heated from 50^{o}C to 800^{o}C using the dynamic rate high resolution mode (TGA 2950, TA Instruments – Res. 5). This procedure was adopted from Bish and Duffy (1990). The results of the XRD and TGA analyses along with other soil characterization data are given in Appendix A.

8.2.4 CEC and Soil pH Determination

Cation exchange capacity (CEC) and soil pH were determined by the Clemson University agricultural extension service. In order to determine the CEC of each soil sample, the soils were buffered to a pH of 8.00. The amount of H, K, Mg, Ca, and Na were then determined in milliequivalents per 100 g of soil. The CEC was then calculated as the sum these values.

For soil pH determination, approximately 15 g of each soil were collected in paper cups. An automatic pipette was then used to add 15.0 mL of deionized water with enough force to mix thoroughly. The samples were allowed to stand for at least one hour. An AS-3000 Dual

pH Analyzer was then used to measure the pH of the resulting solution. Calibration standards and repeated samples were used to verify the results and maintain quality assurance.

8.3 SIMPLE AND MULTIPLE REGRESSION ANALYSES

The final aspect of this investigation was the development of useful models for K_d that utilize common chemical parameters. These models were developed using soil pH, CEC, clay percentage, aluminum content, iron content, manganese content, and titanium content. Model parameters were derived with the aid of the SAS statistical program. Models were developed by first identifying the parameters for which the K_d values for each isotope showed a significant correlation. Those parameters that displayed correlation coefficients of about 0.25 or greater using the correlation procedure in SAS were added to the list of possible model parameters along with any other parameters that may have been identified in the literature review. Using the selected parameters, all possible regressions were examined, and the overall best model for each radionuclide was chosen on the basis of model adequacy measures such as the adjusted R^2 value, the C_p value, and the p-value for the global F-test. The adjusted R^2 value is an indication of the fraction of variability in the data that can be accounted for by the model being utilized after adjustment for the number of variables used in the model input. The C_p value is a model selection criterion designed to minimize the total mean square error and regression bias. In general, the C_p value should be a small value close to $p + 1$, where p is the number of input variables. The global F-test is a statistical significance test designed to test whether or not a model is adequate for providing information about the system being modeled. The p-value for this test indicates the highest significance level at which the model can be said to be useful. The principle of parsimony, which dictates that when only small improvements can be made the best model will have the fewest number of parameters possible, was also taken into account. The model parameters that were ultimately utilized were soil CEC (meq/100g), Clay %, Al content (ppm), Fe content (ppm), and Ti content (ppm).

8.4 REFERENCES FOR APPENDIX A

Bish, D.L., and C.J. Duffy. 1990. Thermogravimetric analysis of minerals, p. 95-157, *In* J. W. Stucki and D. L. Bish, eds. Thermal analysis in clay science, Vol. 3. Clay Minerals Society, Boulder, CO.

Brindley, G.W., and G. Brown. 1980. Crystal structures of clay minerals and their identification by X-ray diffraction Mineralogical Society, London.

Drever, J.I. 1973. The preparation of oriented clay mineral specimens for x-ray diffraction analysis by a filter membrane peel technique. American Mineralogist 58:553-554.

Jackson, M.L. 1979. *Soil Chemical Analysis- Advanced Course.* 2nd edition ed. Published by the author, Madison, WI.

Krupka, K. M., D. I. Kaplan, G. Whelan, R. J. Serne, and S. V. Mattigod. 199a9. Understanding Variation in Partition Coefficient, Kd, Values. Volume 1: The Kd Model, Methods of Measurement, and Application of Chemical Reaction Codes. EPA 402-R-99-004A. Office of Air and Radiation, Office of Solid Waste and Emergency Response, U.S. Environmental Protection Agency, Washington, DC. (http://www.epa.gov/radiation/cleanup/partition.htm)

Krupka, K. M., D. I. Kaplan, G. Whelan, R. J. Serne, and S. V. Mattigod. 1999b. Understanding Variation in Partition Coefficient, Kd, Values. Volume II: Review of Geochemistry and Available Kd Values, for Cadmium, Cesium, Chromium, Lead, Plutonium, Radon, Strontium, Thorium, Tritium (3H), and Uranium. EPA 402-R-99-004A. Office of Air and Radiation, Office of Solid Waste and Emergency Response, U.S. Environmental Protection Agency, Washington, DC.

Lee, S.-Z., Chang, L., Chen, C.-M., Tsai, Y.I., and Liu, M.-C. 2001. Predicting soil-water Los Alamos National Laboratory. Periodic Table. Yttrium. Accessed August 15, 2007 http://periodic.lanl.gov/elements/39.html.

Whittig, L.D., and W.R. Allardice. 1986. X-ray diffraction techniques, p. 331-362, *In* A. Klute, ed. Methods of soil analysis, Part 1. Physical and mineralogical methods. ASA, Madison, WI.

9.0 APPENDIX B: SOIL CHARACTERIZATION DATA

Table B.1. Summary of soil characterization data

Sample Depth (ft)	CEC (meq/100g)	Soil pH	Avg. Clay %	Al (ppm)	Ti (ppm)	Mn (ppm)	Fe (ppm)
BGO-3A							
-11	2.0	5.1	21.16	1510	14	2	4272
-12.5	1.6	5.1	19.45	1424	9	2	2310
-15	2.7	6.0	29.05	1550	6	11	5062
-17.5	3.3	5.0	49.73	2168	7	4	10183
-20	1.5	4.9	18.48	1173	6	11	3554
-25	3.2	5.8	22.71	2240	15	1731	24698
-27	1.2	5.0	14.62	1255	10	18	716
-30	1.4	5.3	11.56	1104	7	27	429
-32	1.0	5.3	7.00	1237	11	7	581
-35	1.1	5.4	8.76	1525	7	9	594
-38	1.0	5.2	6.31	1601	15	12	814
-40	1.6	5.3	9.70	922	6	6	410
-42	1.0	5.2	7.16	892	4	34	209
-45	1.0	5.2	7.73	1102	6	3	260
-47	1.5	5.2	9.16	1223	12	3	327
-50	1.6	5.0	9.57	1114	7	3	253
-53	1.4	4.9	9.74	1125	6	3	288
-55	1.5	5.1	11.03	1161	8	9	363
-58	1.1	6.0	2.16	1057	24	11	1160
-60	1.0	6.4	0.31	1148	9	20	589
-70	1.6	5.0	6.60	1377	14	5	2223
-75	1.6	4.8	3.70	1291	9	5	3015
-80	1.2	6.0	2.32	1926	31	27	13619
-85	1.1	5.8	1.18	1723	16	14	6566
-90	2.9	5.3	7.94	2754	58	169	22696
-95	9.3	4.9	21.51	2498	6	204	10462
-100	7.4	5.1	12.32	1727	14	47	2991

Soil pH and CEC were determined by the Clemson University Agricultural Extension Service. Clay percentage, Al, Fe, Mn, and Ti content were determined with the assistance of Dr. John Seaman of the Savannah River Ecology Laboratory.

Table B.2. Clay mineralogy based on XRD and TGA analysis.

Sample Depth (ft)	Clay Mineralogy[(a)]
17.5	kaol(53%)>illite
42	kaol(62%)>illite
80	goe(29%)>kaol(18%)≈smec
90	smec>goe(21%)≈kaol(18%)>ill
95	smec>kaol(27%)>ill>goe
100	smec>kaol

goe= goethite, kaol = kaolinite, ill = illite or weathered mica, smec = smectite

Percent composition was estimated from standard thermal weight loss for ideal clay minerals (Jackson, 1979).

10.0 APPENDIX C: SUB-SURFACE K_d PROFILES AND QUALTIY ASSURANCE (GAMMA RAY STANDARDS AND MASS BALANCE FOR K_d MEASUREMENTS)

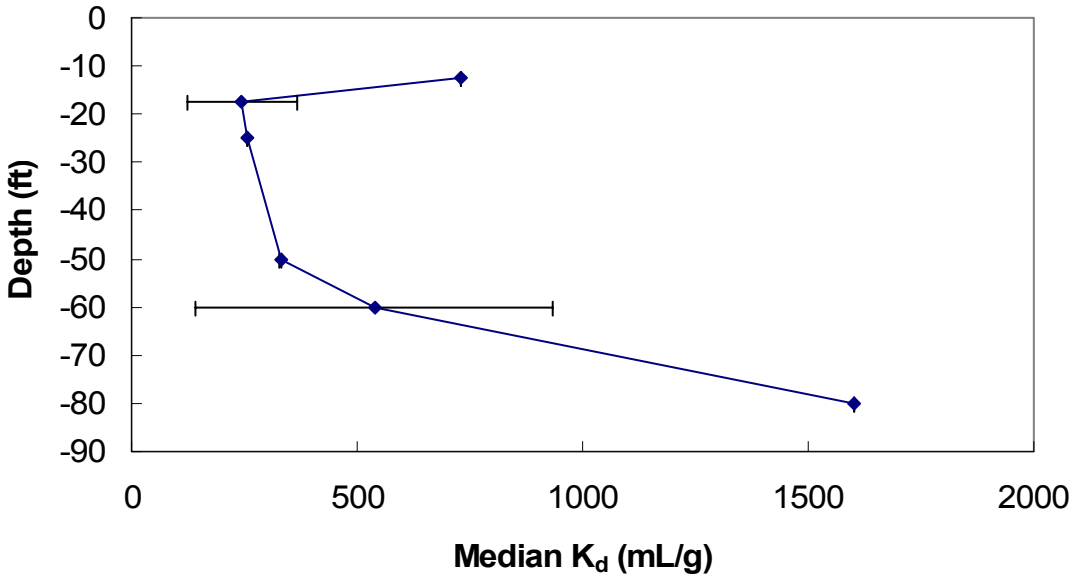

Figure C.1. Sub-surface K_d profile for ^{241}Am

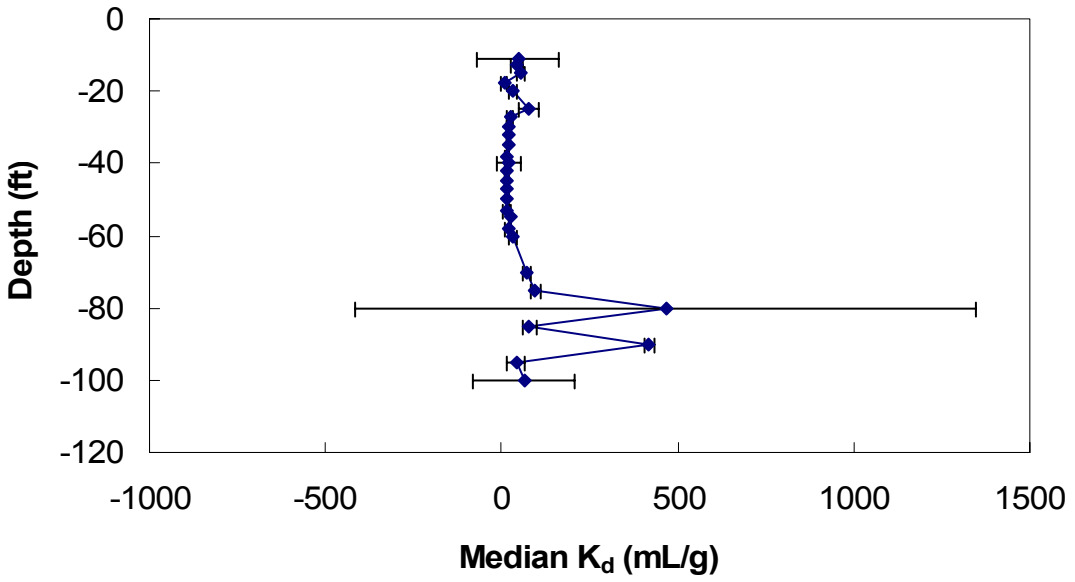

Figure C.2. Sub-surface K_d profile for ^{109}Cd

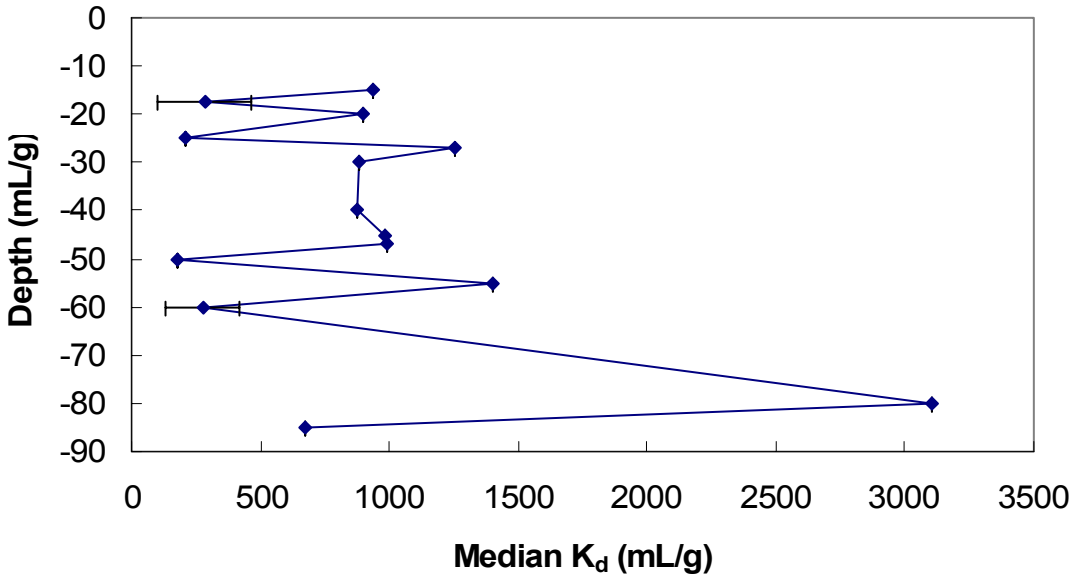

Figure C.3. Sub-surface K_d profile for ^{139}Ce

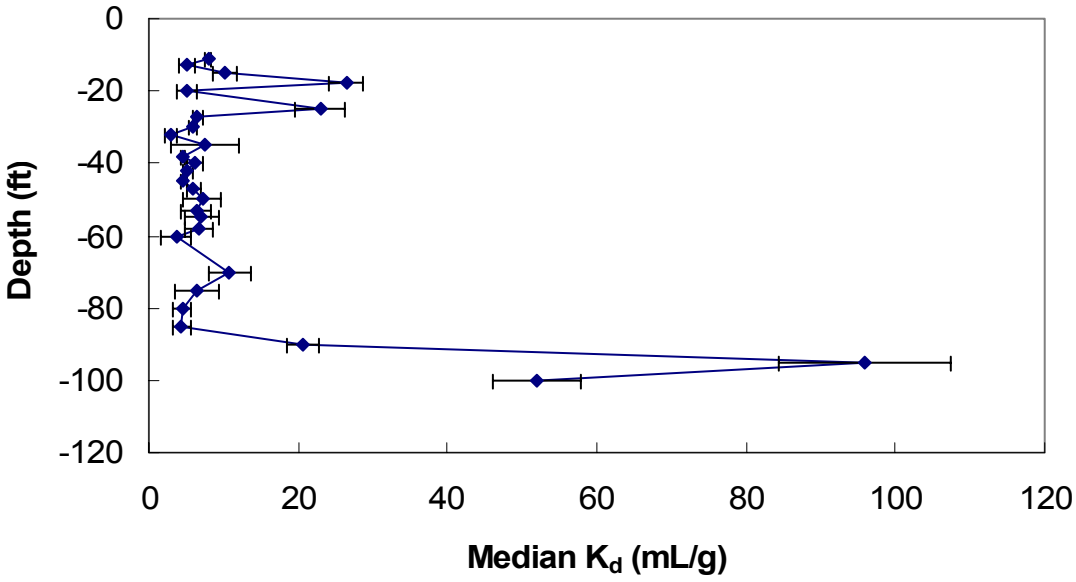

Figure C.4. Sub-surface K_d profile for ^{137}Cs

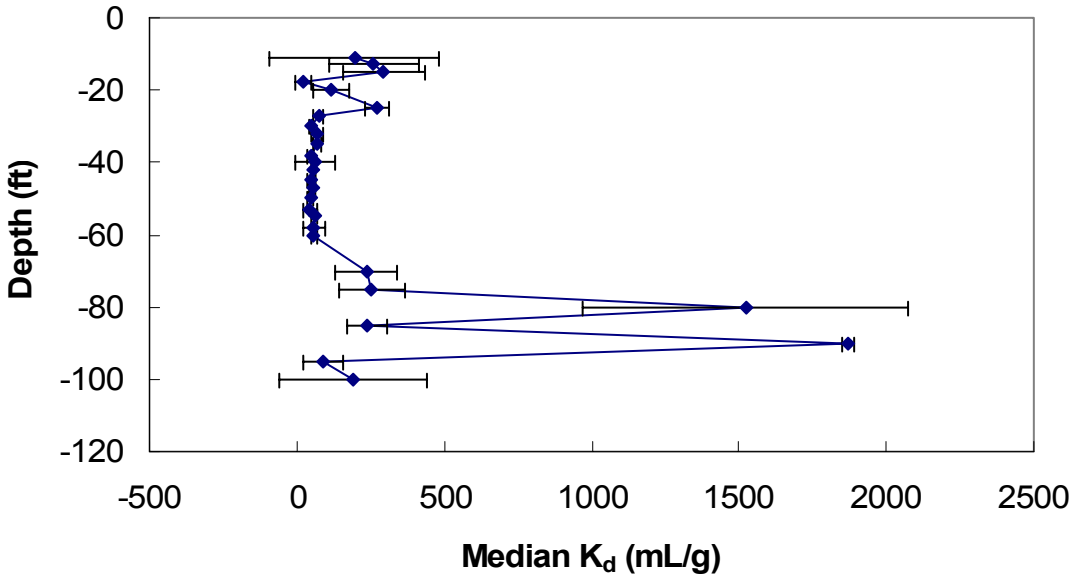

Figure C.5. Sub-surface K_d profile for ^{57}Co

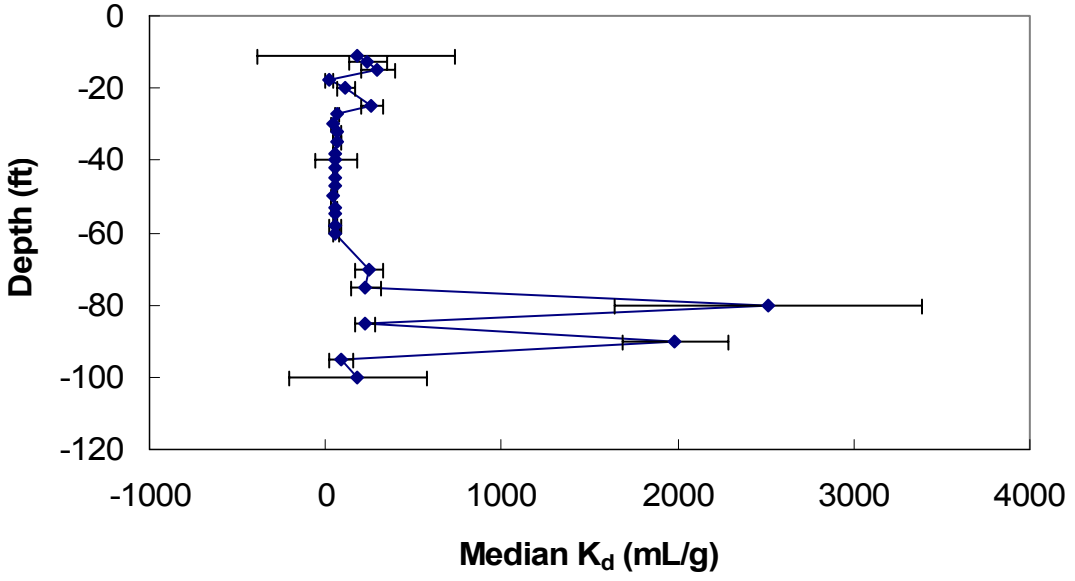

Figure C.6. Sub-surface K_d profile for ^{60}Co

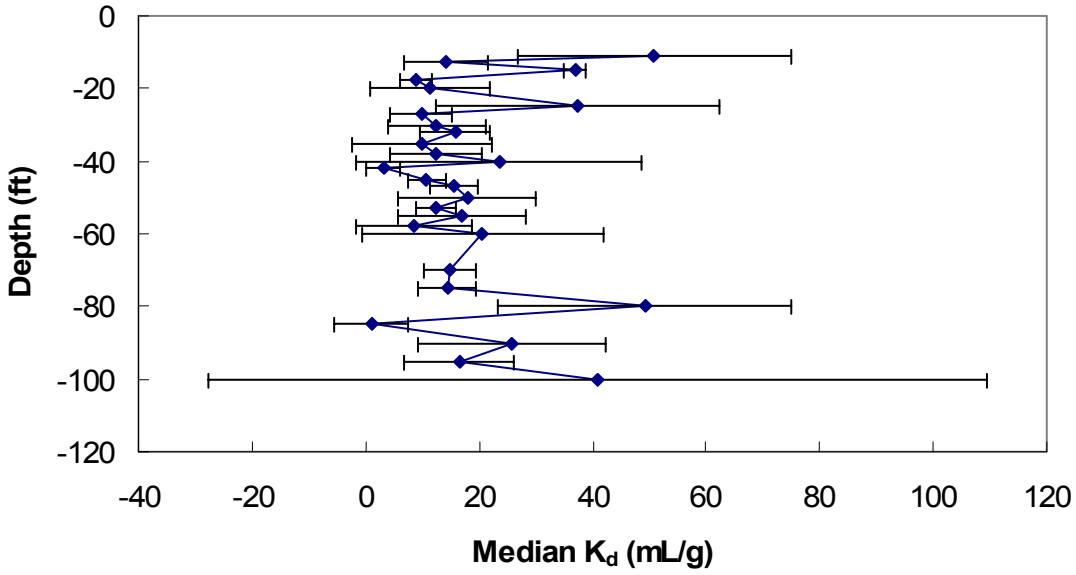

Figure C.7. Sub-surface K_d profile for ^{203}Hg

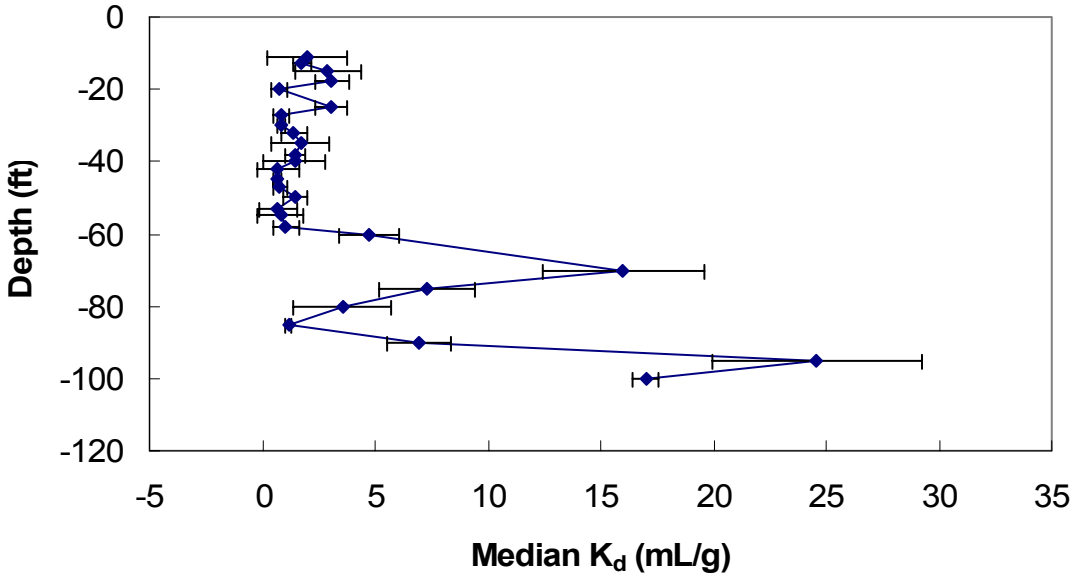

Figure C.8. Sub-surface K_d profile for ^{85}Sr

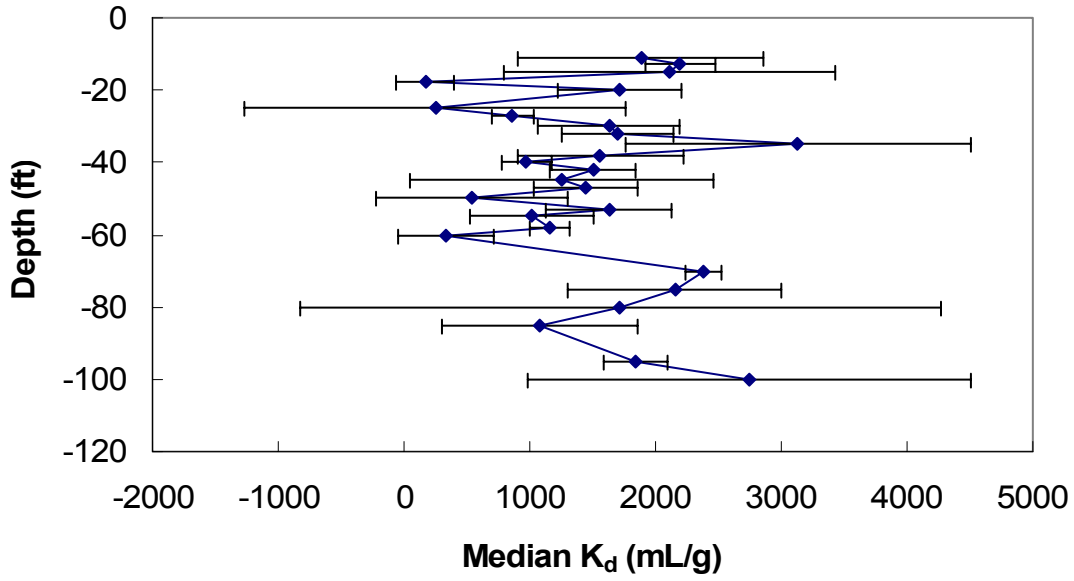

Figure C.9. Sub-surface K_d profile for ^{88}Y

10.1 DESCRIPTION OF MIXED GAMMA-RAY STANDARD

The mixed gamma-ray standard contained 50 mL of acidified (HCl) radionuclide solution. The solution was contained within a flame-sealed glass vial and was calibrated April 1, 2006. The component radionuclides and their corresponding activity levels are listed in Table C.1.

Table C.1. Mixed gamma-ray standard description

Radionuclide	Activity (μCi)	Radionuclide	Energy (keV)	Activity (gammas per second)
^{109}Cd	2	^{241}Am	58.5	2042
^{57}Co	0.044	^{109}Cd	87.4	2684
^{139}Ce	0.066	^{57}Co	121.5	1396
^{203}Hg	0.14	^{139}Ce	165.4	1964
^{113}Sn	0.12	^{203}Hg	279.2	4311
^{137}Cs	0.055	^{113}Sn	392.1	2933
^{88}Y	0.2	^{85}Sr	514.3	5374
^{60}Co	0.09	^{137}Cs	662.9	1740
^{241}Am	0.15	^{88}Y	899.4	6985
^{85}Sr	0.15	^{60}Co	1174.1	3327
		^{60}Co	1332.8	3360
Total Activity	3.015	^{88}Y	1833.7	7267

10.2 REPRESENTATIVE MASS BALANCE FOR BATCH SORPTION PROCEDURE

Table C.2. Representative* mass balance obtained for radionuclides utilized in the batch sorption process

Radionuclide	Mass Balance Fraction	Uncertainty
Am-241	1.101	0.007
Cd-109	0.991	0.006
Co-57	1.008	0.009
Ce-139	1.103	0.011
Hg-203	0.880	0.014
Sn-113	1.088	0.013
Sr-85	1.002	0.003
Cs-137	0.886	0.010
Y-88	1.116	0.013
Co-60	1.072	0.012
Co-60	1.033	0.013
Y-88	1.084	0.017

*Obtained for the first trial of the 15 ft depth of the BGO-3A core

11.0 APPENDIX D: K_d VALUE PROBABILITY PLOTS FOR ENTIRE CORE

11.1 UNSTRATIFIED CORE NORMAL PROBABILITY PLOTS

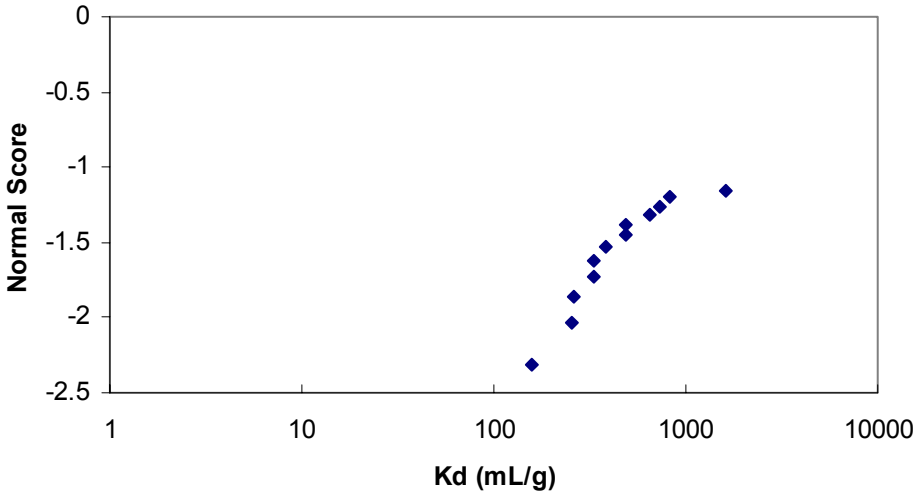

Figure D.1: Normal probability plot of K_d for ^{241}Am.

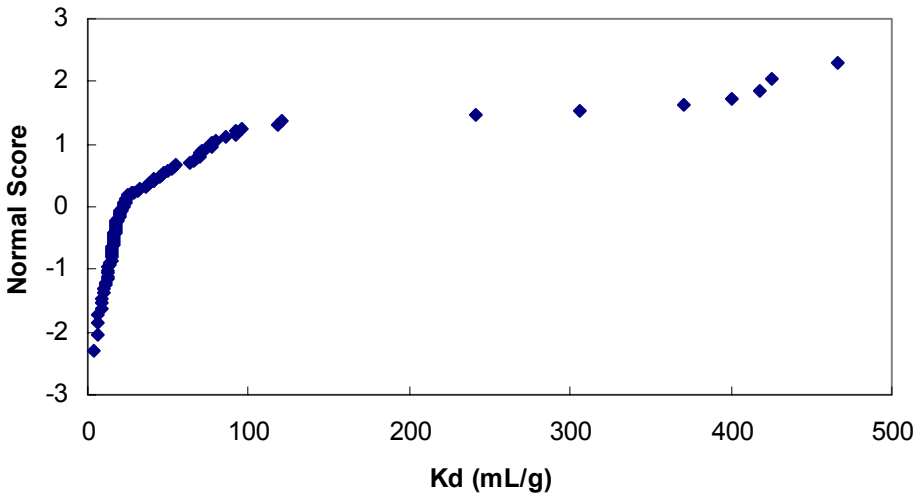

Figure D.2: Normal probability plot of K_d for ^{109}Cd.

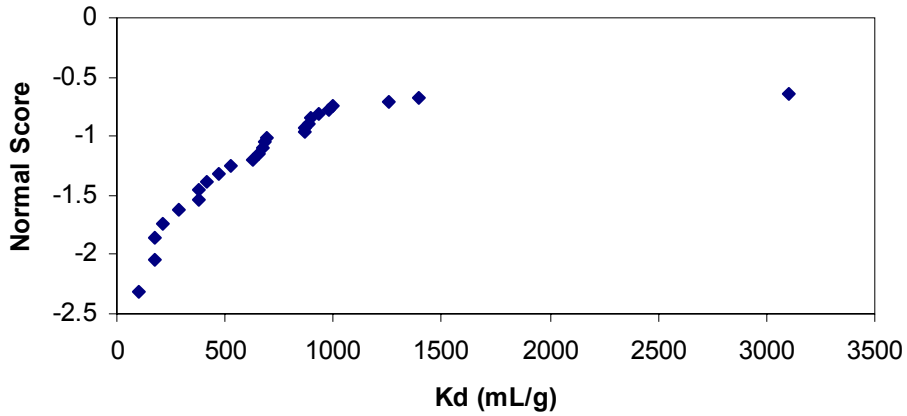

Figure D.3: Normal probability plot of K_d for ^{139}Ce.

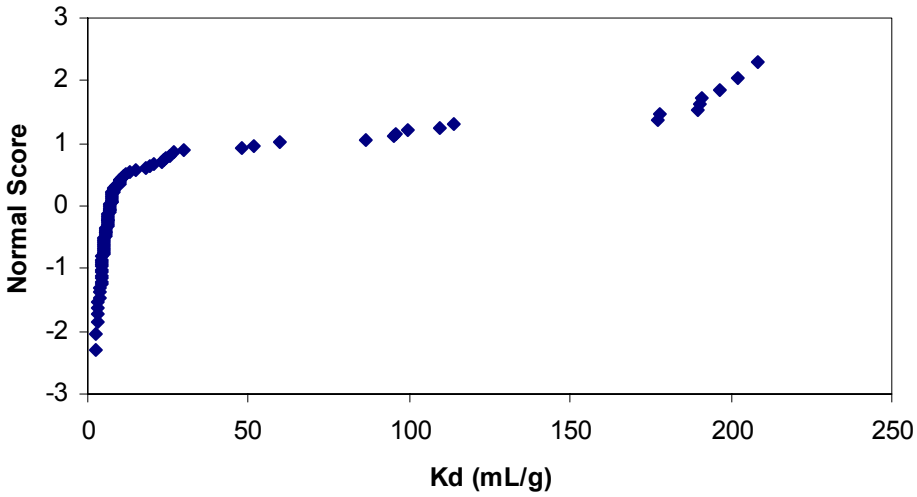

Figure D.4: Normal probability plot of K_d for ^{137}Cs.

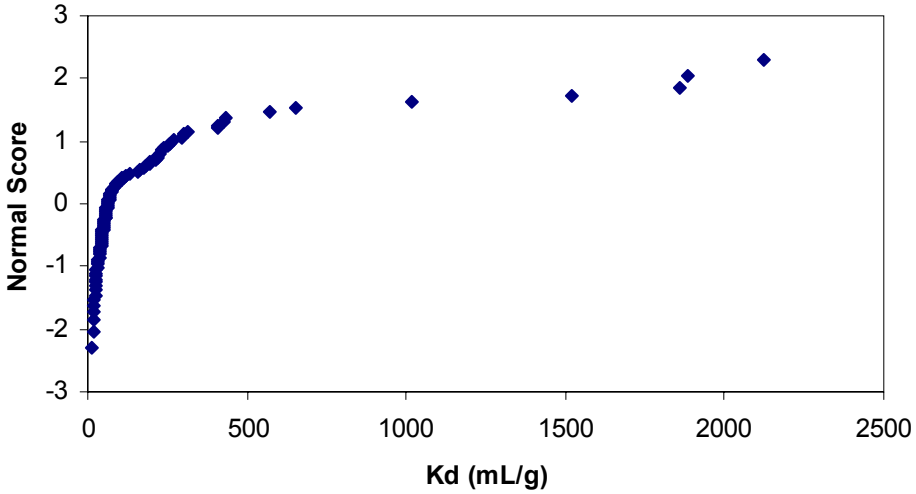

Figure D.5: Normal probability plot of K_d for ^{57}Co.

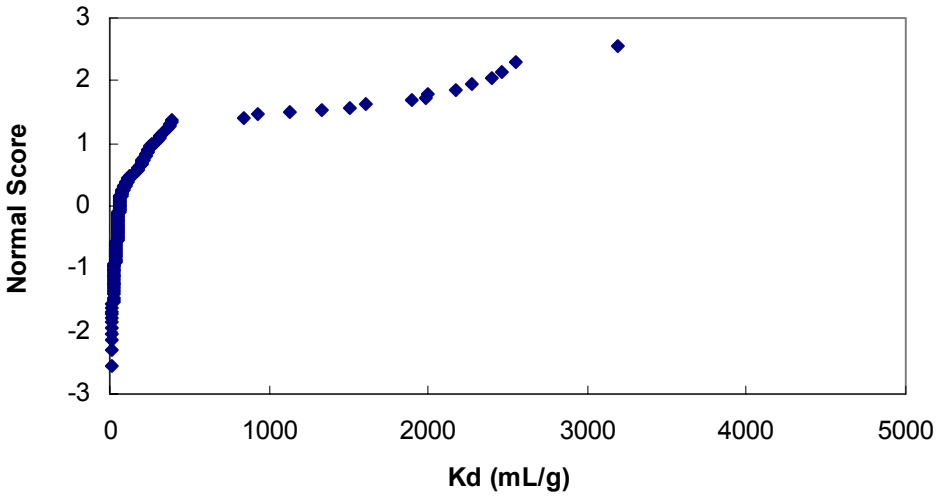

Figure D.6: Normal probability plot of K_d for ^{60}Co.

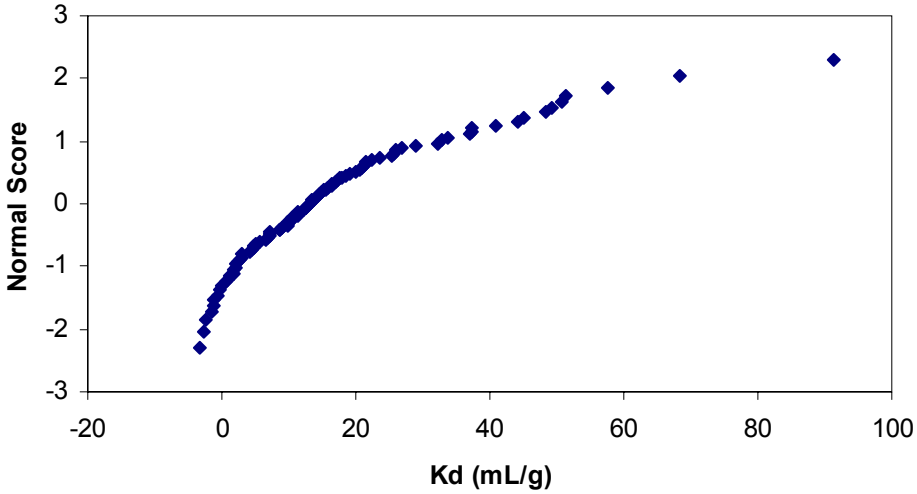

Figure D.7: Normal probability plot of K_d for ^{203}Hg.

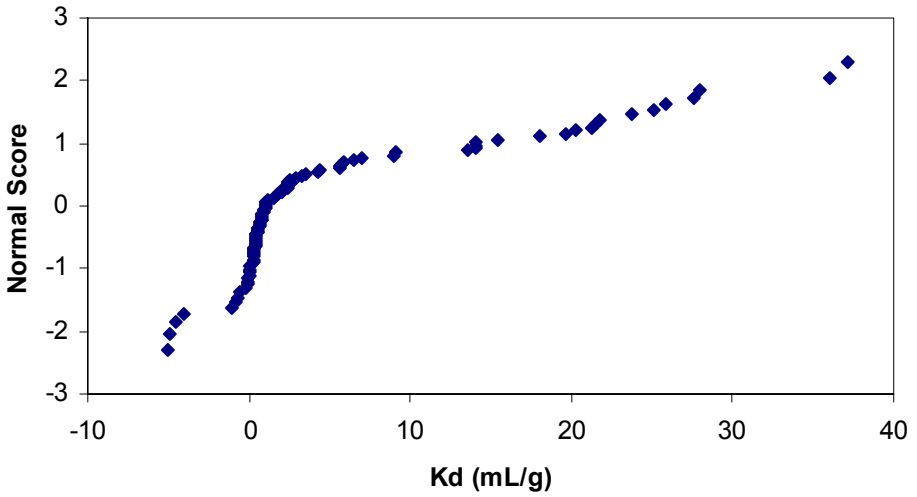

Figure D.8: Normal probability plot of K_d for ^{85}Sr.

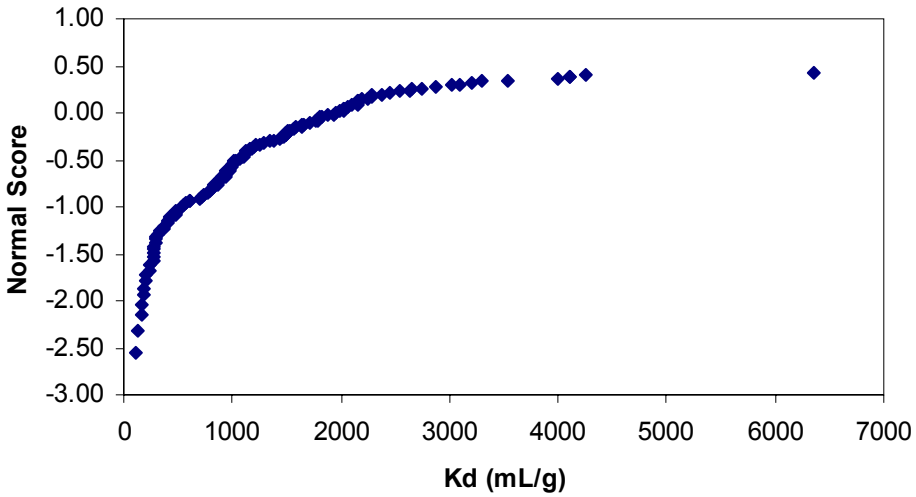

Figure D.9: Normal probability plot of K_d for ^{88}Y.

12.0 APPENDIX E: VISUAL MINTEQ ANALYSIS

Table E.1. Species distribution of radionuclides present in the spiked and neutralized groundwater solution

Component	% of total component concentration	Species
Cd+2	90.43	Cd+2
	8.80	Cd DOM1
	0.05	CdOH+
	0.62	CdCl+
	0.10	CdSO4 (aq)
Co+2	99.71	Co+2
	0.19	CoOH+
	0.09	CoSO4 (aq)
Ce+3	93.84	Ce+3
	4.47	CeOH+2
	0.03	CeCl+2
	1.66	CeSO4+
Cs+1	99.99	Cs+1
Y+3	83.20	Y+3
	15.76	YOH+2
	0.02	YCl+2
	1.01	YSO4+
Am+3	21.00	Am+3
	15.40	Am(OH)2+
	63.05	AmOH+2
	0.55	AmSO4+
Sr+2	99.89	Sr+2
	0.01	SrCl+
	0.09	SrSO4 (aq)

DISTRIBUTION

Savannah River Site

B. T. Butcher	773-43A, Rm. 216
L. B. Collard	773-43A, Rm. 207
J. R. Cook	773-43A, Rm. 209
M. E. Denham	773-42A, Rm. 218
G. P. Flach	773-42A, Rm. 211
W. T. Goldston	705-3C, Rm. 105
J. C. Griffin	773A, Rm. A-231
L. L. Hamm	773-42A, Rm. 145
R. A. Hiergesell	773-42A, Rm. 251
D. I. Kaplan (3 copies)	773-43A, Rm. 215
E. P. Shine	773-42A, Rm. 133
G. A. Taylor	773-41A, Rm. 156
E. L. Wilhite	773-43A, Rm. 214
WPT File (2 copies)	773-43A, Rm. 213
STI (3 copies)	703-43A

Clemson University, Environmental Engineering and Earth Sciences Department

C. M. Coates
T. DeVol
R. A. Fjeld
K. Grogan

Savannah River Ecology Laboratory, University of Georgia

J. C. Seaman	737-A, Rm. 155